Inorganic Chemistry

Article

pubs.acs.org/IC

Phosphorescent Cellular Probes and Uptake Indicators Derived from Cyclometalated Iridium(III) Bipyridine Complexes Appended with a Glucose or Galactose Entity

Wendell Ho-Tin Law, Lawrence Cho-Cheung Lee, Man-Wai Louie, Hua-Wei Liu, Tim Wai-Hung Ang, and Kenneth Kam-Wing Lo*

Institute of Molecular Functional Materials [Areas of Excellence Scheme, University Grants Committee (Hong Kong)] and Department of Biology and Chemistry, City University of Hong Kong, Tat Chee Avenue, Kowloon, Hong Kong, P. R. China

Supporting Information

ABSTRACT: A series of phosphorescent cyclometalated iridium(III) polypyridine complexes appended with a β-D-glucose moiety $[Ir(N^C)_2(bpy\text{-}TEG\text{-}ONCH_3\text{-}\beta\text{-}D\text{-}glc)](PF_6)$ [bpy-TEG-ONCH$_3$-β-D-glc = 4-(10-*N*-methyl-*N*-(β-D-glucopyranosyl)-amino-oxy-2,5,8-trioxa-dec-1-yl)-4′-methyl-2,2′-bipyridine; HN^C = 2-((1,1′-biphenyl)-4-yl)benzothiazole) (Hbt) (**1a**), 2-phenylpyridine (Hppy) (**2a**), 2-phenylquinoline (Hpq) (**3a**), 7,8-benzoquinoline (Hbzq) (**4a**)] has been synthesized and characterized. The D-galactose counterparts $[Ir(N^C)_2(bpy\text{-}TEG\text{-}ONCH_3\text{-}\beta\text{-}D\text{-}gal)](PF_6)$ [bpy-TEG-ONCH$_3$-β-D-gal = 4-(10-*N*-methyl-*N*-(β-D-galactopyranosyl)-amino-oxy-2,5,8-trioxa-dec-1-yl)-4′-methyl-2,2′-bipyridine; HN^C = Hbt (**1b**), Hppy (**2b**), Hpq (**3b**), Hbzq (**4b**)] and a sugar-free bt complex $[Ir(bt)_2(bpy\text{-}TEG\text{-}OMe)](PF_6)$ [bpy-TEG-OMe = 4-(2,5,8,11-tetraoxa-dodec-1-yl)-4′-methyl-2,2′-bipyridine] (**1c**) have also been prepared. Upon photoexcitation, all the complexes displayed intense and long-lived triplet metal-to-ligand charge-transfer (^{3}MLCT) [$d\pi(Ir) \rightarrow \pi^*(N^N)$] or triplet intraligand (^{3}IL) ($\pi \rightarrow \pi^*$) (N^C and N^N) emission. The lipophilicity, the cellular uptake efficiency, and cytotoxicity of the complexes toward human cervix epithelioid carcinoma cells (HeLa) have been examined. Temperature dependence and chemical inhibition experiments indicated that the transport of bt−glucose complex **1a** across the cell membrane occurred through an energy-requiring process such as endocytosis, in additional to a pathway that was mediated by glucose transporters (GLUTs). Importantly, the cellular uptake efficiency of this complex was found to be strongly dependent on hormonal stimulation and inhibition, rendering it a new phosphorescent metabolic indicator. Additionally, laser-scanning confocal microscopy revealed that the complex was localized in the mitochondria and highly resistant to photobleaching compared to a fluorescent organic glucose derivative 2-(*N*-(7-nitrobenz-2-oxa-1,3-diazol-4-yl)amino)-2-deoxy-D-glucose (2-NBDG).

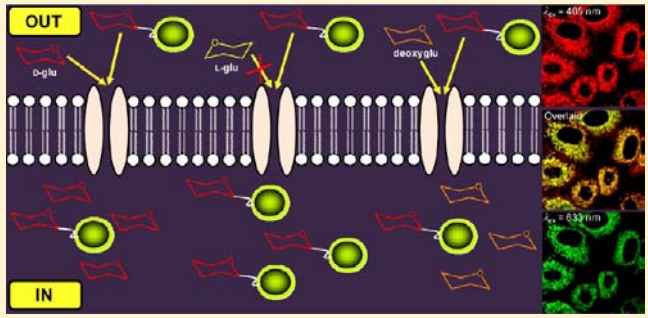

INTRODUCTION

Glucose is essential to mammalian cells because it is not only a precursor of glycoproteins, triglycerides, and glycogen but also a crucial energy source through the generation of adenosine triphosphate (ATP).[1] Specific membrane carrier proteins glucose transporters (GLUTs) and Na^+/glucose cotransporters (SGLTs) are known to mediate the passive facilitative and the energy-dependent transport of relatively hydrophilic glucose through the lipid bilayers, respectively.[1c,e,2] In particular, most cancer cells show an increased rate of glucose uptake and metabolism, and a higher demand for glucose is usually reflected by the overexpression of various GLUTs in these cells.[1c,2b,3] Thus, glucose derivatives with a reporter functionality have been used to study glucose uptake, examine metabolism of cells, and image tumor tissues. Although radioactive ^{18}F-labeled 2-fluoro-2-deoxy-D-glucose (^{18}F-FDG) is the most common imaging reagent,[4] the use of fluorescent sugar derivatives coupled with optical methods such as laser-scanning confocal microscopy has emerged as an attractive alternative because excellent spatial and temporal resolution can be achieved in real time.[5] Fluorescent dyes appended with a D-glucose pendant have been utilized to study glucose uptake by cells and imaging of cancer tissues; examples include 2-dansylglucosamine,[6a] 2-NBDG,[6b,c] Cy3-2DG,[6d,e] and the near-IR and two-photon absorbing derivatives such as Cy5.5-2DG,[7a] IRDye 800CW-2DG,[7b] CyNE 2-DG,[7c] Pyro-2DG,[7d] and AG2.[7e] Despite the fact that transition metal sugar complexes have been reported,[8,9] those exhibiting phosphorescence properties are very limited, and their use in cellular studies has not been extensively explored.[9]

With our ongoing interest in phosphorescent cyclometalated iridium(III) polypyridine complexes as biological probes and imaging reagents,[10] we envisage that modification of these complexes with a D-glucose entity will generate a new class of phosphorescent probes, which can be exploited as cellular uptake indicators. Herein, we report the synthesis, characterization, photophysical properties, and lipophilicity of a series of

Received: July 4, 2013
Published: November 5, 2013

   dx.doi.org/10.1021/ic401714p | *Inorg. Chem.* 2013, 52, 13029−13041

phosphorescent cyclometalated iridium(III) bipyridine D-glucose complexes $[Ir(N^{\wedge}C)_2(bpy\text{-}TEG\text{-}ONCH_3\text{-}\beta\text{-}D\text{-}glc)](PF_6)$ [bpy-TEG-$ONCH_3$-β-D-glc = 4-(10-*N*-methyl-*N*-(β-D-glucopyranosyl)-amino-oxy-2,5,8-trioxa-dec-1-yl)-4′-methyl-2,2′-bipyridine; HN^C = 2-((1,1′-biphenyl)-4-yl)benzothiazole) (Hbt) (**1a**), 2-phenylpyridine (Hppy) (**2a**), 2-phenylquinoline (Hpq) (**3a**), 7,8-benzoquinoline (Hbzq) (**4a**)] (Chart 1). Their D-galactose counterparts

Chart 1. Structures of the Iridium(III) Complexes

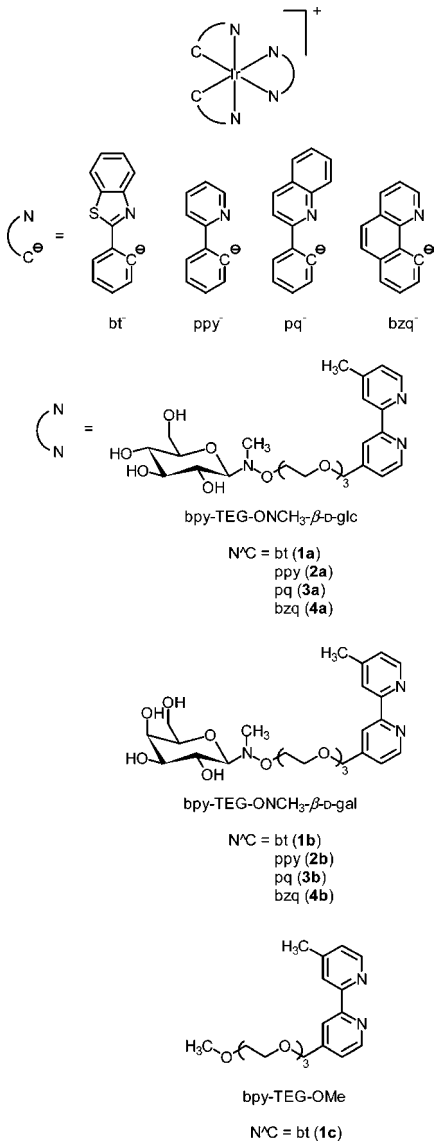

$[Ir(N^{\wedge}C)_2(bpy\text{-}TEG\text{-}ONCH_3\text{-}\beta\text{-}D\text{-}gal)](PF_6)$ [bpy-TEG-$ONCH_3$-β-D-gal = 4-(10-*N*-methyl-*N*-(β-D-galactopyranosyl)-amino-oxy-2,5,8-trioxa-dec-1-yl)-4′-methyl-2,2′-bipyridine; HN^C = Hbt (**1b**), Hppy (**2b**), Hpq (**3b**), Hbzq (**4b**)] and a sugar-free bt complex $[Ir(bt)_2(bpy\text{-}TEG\text{-}OMe)](PF_6)$ [bpy-TEG-OMe = 4-(2,5,8,11-tetraoxa-dodec-1-yl)-4′-methyl-2,2′-bipyridine] (**1c**) (Chart 1) have also been prepared for comparison studies. The cellular uptake efficiency and cytotoxicity of these complexes have been studied by ICP-MS and the 3-(4,5-dimethyl-2-thiazolyl)-2,5-diphenyltetrazolium bromide (MTT) assay, respectively. The effects of various inhibitors and biomolecules on the cellular uptake properties of the bt complexes **1a**−**1c** have also been examined. Furthermore, the intracellular distribution and photostability of complex **1a** have been investigated by laser-scanning confocal microscopy.

EXPERIMENTAL SECTION

Materials and Synthesis. All solvents were of analytical grade and purified according to standard procedures.[11] All buffer components were of biological grade and used as received. 4,4′-Dimethyl-2,2′-bipyridine, SeO_2, $IrCl_3{\cdot}3H_2O$, Hbt, Hppy, Hpq, Hbzq, methanesulfonyl chloride, sodium metabisulfite, and di-*tert*-butyl dicarbonate were obtained from Aldrich. D-Glucose, L-glucose, D-galactose, 2-deoxy-D-glucose, *N*-methylhydroxylamine hydrochloride, sodium bicarbonate, sodium borohydride, sodium hydride, triethylamine, trifluoroacetic acid, tri(ethylene glycol), methyl iodide, KPF_6, cobalt(II) chloride, and magnesium chloride were obtained from Acros. MTT, cisplatin, dexamethasone, 3-isobutyl-1-methylxanthine (IBMX), sodium azide, cytochalasin B, and fasentin were purchased from Sigma. Tris-(hydroxymethyl)methylamine (Tris) was supplied by USB. All these chemicals were used without further purification. $[Ir_2(N^{\wedge}C)_4Cl_2]$ (N^C = Hbt, Hppy, Hbzq),[12] bpy-TEG-OH, bpy-TEG-$ONCH_3$-β-D-glc, bpy-TEG-$ONCH_3$-β-D-gal, $[Ir(pq)_2(N^{\wedge}N)](PF_6)$ (N^N = bpy-TEG-$ONCH_3$-β-D-glc, bpy-TEG-$ONCH_3$-β-D-gal) were prepared as previously described.[10c] Insulin, wortmannin, 17β-estradiol (E2), tamoxifen (Tam), adenosine 5′-triphosphate (ATP) disodium salt, and hexokinase from yeast were purchased from Calbiochem. HeLa, HepG2, MCF-7, MDA-MB-231, HEK293T, NIH/3T3, and 3T3-L1 cells were obtained from American Type Culture Collection. High glucose Dulbecco's modified Eagle's medium (DMEM), glucose-free DMEM, fetal bovine serum (FBS), phosphate buffered saline (PBS), trypsin-EDTA, penicillin/streptomycin, MitoTracker Deep Red, and 2-NBDG were purchased from Invitrogen.

Bpy-TEG-OMe. Sodium hydride (56 mg, 2.30 mmol, 60% w/w in mineral oil) was added to a solution of bpy-TEG-OH[10c] (384 mg, 1.20 mmol) in dry DMF (10 mL) at 0 °C under an inert atmosphere of nitrogen. After the mixture was stirred for 30 min, methyl iodide (300 μL, 4.82 mmol) was added at room temperature, and then the mixture was stirred for another 12 h. Cold water (500 μL) was added to quench the reaction. The solvent was removed by evaporation under reduced pressure. The crude product was purified by column chromatography on silica gel using CH_2Cl_2/MeOH/$NH_3{\cdot}H_2O$ (10:1:0.1, v/v/v) as the eluent. The product bpy-TEG-OMe was subsequently isolated as a pale yellow oil. Yield: 247 mg (62%). ^{1}H NMR (300 MHz, $CDCl_3$, 298K, TMS): δ 8.57 (d, J = 5.1 Hz, 1H, H6 of bpy), 8.46 (d, J = 4.8 Hz, 1H, H6′ of bpy), 8.25 (s, 1H, H3 of bpy), 8.16 (s, 1H, H3′ of bpy), 7.29 (d, J = 5.4 Hz, 1H, H5 of bpy), 7.05 (d, J = 6.0 Hz, 1H, H5′ of bpy), 4.55 (s, 2H, CH_2 on C4 of bpy), 3.59−3.52 (m, 10H, CH_2O), 3.44−3.42 (m, 2H, CH_2O) 3.24 (s, 3H, OCH_3), 2.30 (s, 3H, CH_3 of bpy). MS (ESI$^+$): m/z 347 $[M + H]^+$.

[Ir(bt)$_2$(bpy-TEG-ONCH$_3$-β-D-glc)](PF$_6$) (1a). A mixture of $[Ir_2(bt)_4Cl_2]$ (123 mg, 94.9 μmol) and bpy-TEG-$ONCH_3$-β-D-glc[10c] (119 mg, 0.23 mmol) in CH_2Cl_2 was stirred under an inert atmosphere of nitrogen in the dark for 12 h. KPF_6 (46 mg, 0.25 mmol) was added to the mixture, and it was stirred for 30 min and then evaporated to dryness. Subsequent recrystallization of the solid from CH_2Cl_2/diethyl ether afforded complex **1** as yellow crystals. Yield: 184 mg (63%). ^{1}H NMR (400 MHz, CD_3OD, 298 K, TMS): δ 8.66 (s, 1H, H3 of bpy), 8.58 (s, 1H, H3′ of bpy), 8.11 (d, J = 5.6 Hz, 1H, H5 of bpy), 8.04 (d, J = 8.0 Hz, 2H, H4 of benzothiazole ring of bt), 8.00 (d, J = 5.6 Hz, 1H, H5′ of bpy), 7.95−7.92 (m, 2H, H6 of phenyl ring of bt), 7.66 (d, J = 5.6 Hz, 1H, H6 of bpy), 7.49 (d, J = 6.0 Hz, 1H, H6′ of bpy), 7.40 (t, J = 8.0 Hz, 2H, H5 of benzothiazole ring of bt), 7.16−7.10 (m, 4H, H6 of benzothiazole ring and H5 of phenyl ring of bt), 6.89 (t, J = 7.6 Hz, 2H, H4 of phenyl ring of bt), 6.40 (dd, J = 7.6, 4.0 Hz, 2H, H3 of phenyl ring of bt), 6.31 (t, J = 8.8 Hz, 2H, H7 of benzothiazole ring of bt), 4.83 (s, 2H, CH_2 on C4 of bpy), 3.98 (dd, J = 8.8, 3.6 Hz, 1H, H1 of glucose), 3.83−3.58 (m, 14H, H6 of glucose and CH_2O), 3.43 (dt, J = 8.0, 1.2 Hz, 1H, H2 of glucose), 3.36 (t, J = 8.4 Hz, 1H, H3 of glucose), 3.27 (d, J = 8.8 Hz, 1H, H4 of glucose), 3.23−3.19 (m, 1H, H5 of glucose), 2.68 (s, 3H, CH_3N), 2.61 (s, 3H, CH_3 of bpy). IR (KBr) ν/cm^{-1}: 3416 (O−H), 842 (PF_6^-). MS (ESI$^+$): m/z

dx.doi.org/10.1021/ic401714p | Inorg. Chem. 2013, 52, 13029−13041

1136 [M − PF_6^-]$^+$. Anal. Calcd for $IrC_{51}H_{53}N_5O_9S_2PF_6{\cdot}3H_2O$ (%): C, 45.87; H, 4.45; N, 5.24. Found: C, 46.96; H, 4.47; N, 5.17.

[Ir(bt)$_2$(bpy-TEG-ONCH$_3$-β-D-gal)](PF$_6$) (1b). The synthetic procedure was similar to that of complex **1a** except that bpy-TEG-ONCH$_3$-β-D-gal[10c] (119 mg, 0.23 mmol) was used instead of bpy-TEG-ONCH$_3$-β-D-glc. The complex was isolated as orange-yellow crystals. Yield: 199 mg (68%). ^{1}H NMR (400 MHz, CD_3OD, 298 K, TMS): δ 8.66 (s, 1H, H3 of bpy), 8.57 (s, 1H, H3′ of bpy), 8.11 (d, *J* = 5.6 Hz, 1H, H5 of bpy), 8.04 (d, *J* = 8.8 Hz, 2H, H4 of benzothiazole ring of bt), 8.00 (d, *J* = 5.6 Hz, 1H, H5′ of bpy), 7.95−7.92 (m, 2H, H6 of phenyl ring of bt), 7.67 (d, *J* = 5.6 Hz, 1H, H6 of bpy), 7.49 (d, *J* = 6.4 Hz, 1H, H6′ of bpy), 7.41 (t, *J* = 7.6 Hz, 2H, H5 of benzothiazole ring of bt), 7.17−7.10 (m, 4H, H6 of benzothiazole ring and H5 of phenyl ring of bt), 6.89 (t, *J* = 6.0 Hz, 2H, H4 of phenyl ring of bt), 6.40 (dd, *J* = 7.6, 4.0 Hz, 2H, H3 of phenyl ring of bt), 6.31 (t, *J* = 8.8 Hz, 2H, H7 of benzothiazole ring of bt), 4.84 (s, 2H, CH_2 on C4 of bpy), 3.96 (dd, *J* = 8.8, 4.0 Hz, 1H, H1 of galactose), 3.81−3.45 (m, 18H, H2, H3, H4, H5, and H6 of galactose and CH_2O), 2.67 (s, 3H, CH_3N), 2.61 (s, 3H, CH_3 of bpy). IR (KBr) ν/cm^{-1}: 3422 (O−H), 844 (PF_6^-). MS (ESI$^+$): *m*/*z* 1136 [M − PF_6^-]$^+$. Anal. Calcd for $IrC_{51}H_{53}N_5O_9S_2PF_6{\cdot}2.5H_2O$ (%): C, 46.18; H, 4.41; N, 5.28. Found: C, 46.14; H, 4.12; N, 5.08.

[Ir(bt)$_2$(bpy-TEG-OMe)](PF$_6$) (1c). A mixture of [Ir_2(bt)$_4Cl_2$] (164 mg, 0.13 mmol) and bpy-TEG-OMe (79 mg, 0.23 mmol) in CH_2Cl_2/MeOH (30 mL, 1:1, v/v) was heated to reflux under an inert atmosphere of nitrogen in the dark for 12 h. The mixture was then cooled to room temperature, and KPF_6 (46 mg, 0.25 mmol) was added. The mixture was stirred for 30 min and then evaporated to dryness. Subsequent recrystallization of the solid from CH_2Cl_2/diethyl ether afforded complex **1c** as yellow crystals. Yield: 184 mg (73%). ^{1}H NMR (400 MHz, CD_3OD, 298 K, TMS): δ 8.67 (s, 1H, H3 of bpy), 8.58 (s, 1H, H3′ of bpy), 8.11 (d, *J* = 6.0 Hz, 1H, H5 of bpy), 8.04 (d, *J* = 8.0 Hz, 2H, H4 of benzothiazole ring of bt), 8.00 (d, *J* = 5.6 Hz, 1H, H5′ of bpy), 7.95−7.92 (m, 2H, H6 of phenyl ring of bt), 7.65 (d, *J* = 5.1 Hz, 1H, H6 of bpy), 7.50 (d, *J* = 5.2 Hz, 1H, H6′ of bpy), 7.40 (t, *J* = 8.0 Hz, 2H, H5 of benzothiazole ring of bt), 7.16−7.10 (m, 4H, H6 of benzothiazole ring and H5 of phenyl ring of bt), 6.89 (dt, *J* = 7.6, 1.2 Hz, 2H, H4 of phenyl ring of bt), 6.42−6.39 (m, 2H, H3 of phenyl ring of bt), 6.34−6.29 (m, 2H, H7 of benzothiazole ring of bt), 4.87 (s, 2H, CH_2 on C4 of bpy), 3.76−3.71 (m, 4H, CH_2O), 3.64−3.54 (m, 6H, CH_2O), 3.43−3.40 (m, 2H, CH_2O), 3.19 (s, 3H, OCH_3), 2.61 (s, 3H, CH_3 of bpy). IR (KBr) ν/cm^{-1}: 841 (PF_6^-). MS (ESI$^+$): *m*/*z* 959 [M − PF_6^-]$^+$. Anal. Calcd for $IrC_{45}H_{42}N_4O_4S_2PF_6{\cdot}H_2O$ (%): C, 48.16; H, 3.95; N, 4.99. Found: C, 48.10; H, 4.05; N, 4.90.

[Ir(ppy)$_2$(bpy-TEG-ONCH$_3$-β-D-glc)](PF$_6$) (2a). The synthetic procedure was similar to that of complex **1a** except that [Ir_2(ppy)$_4Cl_2$] (93.5 mg, 87.3 μmol) was used instead of [Ir_2(bt)$_4Cl_2$]. The complex was isolated as bright yellow crystals. Yield: 146 mg (79%). ^{1}H NMR (400 MHz, CD_3OD, 298 K, TMS): δ 8.67 (s, 1H, H3 of bpy), 8.59 (s, 1H, H3′ of bpy), 8.12 (d, *J* = 8.4 Hz, 2H, H3 of pyridyl ring of ppy), 7.95 (d, *J* = 5.6 Hz, 1H, H6 of bpy), 7.88−7.82 (m, 5H, H6′ of bpy, H4 and H6 of pyridyl ring of ppy), 7.64 (t, *J* = 5.2 Hz, 2H, H3 of phenyl ring of ppy), 7.55 (d, *J* = 5.2 Hz, 1H, H5′ of bpy), 7.09−7.01 (m, 4H, H5 of pyridyl ring and H4 of phenyl ring of ppy), 6.89 (t, *J* = 6.8 Hz, 2H, H5 of phenyl ring of ppy), 6.32−6.29 (m, 2H, H6 of phenyl ring of ppy), 4.63 (s, 2H, CH_2 on C4 of bpy), 3.99 (dd, *J* = 8.8, 3.2 Hz, 1H, H1 of glucose), 3.87−3.62 (m, 14H, H6 of glucose and CH_2O), 3.51−3.41 (m, 2H, H2 and H3 of glucose), 3.27 (d, *J* = 8.4 Hz, 1H, H4 of glucose), 3.23−3.19 (m, 1H, H5 of glucose), 2.70 (s, 3H, CH_3N), 2.59 (s, 3H, CH_3 of bpy). IR (KBr) ν/cm^{-1}: 3421 (O−H), 844 (PF_6^-). MS (ESI$^+$): *m*/*z* 1025 [M − PF_6^-]$^+$. Anal. Calcd for $IrC_{47}H_{53}N_5O_9PF_6{\cdot}2H_2O{\cdot}CH_2Cl_2$ (%): C, 44.68; H, 4.61; N, 5.43. Found: C, 44.71; H, 4.68; N, 5.51.

[Ir(ppy)$_2$(bpy-TEG-ONCH$_3$-β-D-gal)](PF$_6$) (2b). The synthetic procedure was similar to that of complex **1b** except that [Ir_2(ppy)$_4Cl_2$] (81.4 mg, 75.9 μmol) was used instead of [Ir_2(bt)$_4Cl_2$]. The complex was isolated as yellow crystals. Yield: 85 mg (48%). ^{1}H NMR (400 MHz, CD_3OD, 298 K, TMS): δ 8.68 (s, 1H, H3 of bpy), 8.59 (s, 1H, H3′ of bpy), 8.13 (d, *J* = 8.0 Hz, 2H, H3 of pyridyl ring of ppy), 7.95 (d, *J* = 5.6 Hz, 1H, H6 of bpy), 7.88−7.82 (m, 5H, H6′ of bpy, H4 and H6 of pyridyl ring of ppy), 7.65 (t, *J* = 4.8 Hz, 2H, H3 of phenyl ring of ppy), 7.56 (d, *J* = 4.8, 1H, H5 of bpy), 7.39 (d, *J* = 5.6 Hz, 1H, H5′ of bpy), 7.09−7.01 (m, 4H, H5 of pyridyl ring and H4 of phenyl ring of ppy), 6.91−6.87 (m, 2H, H5 of phenyl ring of ppy), 6.32−6.29 (m, 2H, H6 of phenyl ring of ppy), 4.64 (s, 2H, CH_2 on C4 of bpy), 3.95 (dd, *J* = 8.8, 2.4 Hz, 1H, H1 of galactose), 3.84−3.46 (m, 18H, H2, H3, H4, H5, H6 of glucose and CH_2O), 2.69 (s, 3H; CH_3N), 2.60 (s, 3H, CH_3 of bpy). IR (KBr) ν/cm^{-1}: 3423 (O−H), 843 (PF_6^-). MS (ESI): *m*/*z* 1025 [M − PF_6^-]$^+$. Anal. Calcd for $IrC_{47}H_{53}N_5O_9PF_6{\cdot}1.5CH_2Cl_2$ (%): C, 44.93; H, 4.35; N, 5.40. Found: C, 44.65; H, 4.65; N, 5.60.

[Ir(pq)$_2$(bpy-TEG-ONCH$_3$-β-D-glc)](PF$_6$) (3a). The synthetic procedure was reported previously.[3] ^{1}H NMR (400 MHz, CD_3OD, 298 K, TMS): δ 8.41−8.39 (m, 4H, H3 of quinoline of pq, H3 and H6 of bpy), 8.26 (s, 1H, H3′ of bpy), 8.18−8.17 (m, 4H, H3 of phenyl ring and H4 of quinoline of pq), 8.08 (d, *J* = 6.0 Hz, 1H, H6′ of bpy), 7.84 (d, *J* = 7.6 Hz, 2H, H8 of quinoline of pq), 7.56 (d, *J* = 6.0 Hz, 1H, H5 of bpy), 7.42−7.38 (m, 5H, H5′ of bpy, H5 and H7 of quinoline of pq), 7.18−7.15 (m, 2H, H4 of phenyl ring of pq), 7.07−7.03 (m, 2H, H6 of quinoline of pq), 6.82−6.79 (m, 2H, H5 of phenyl ring of pq), 6.52−6.49 (m, 2H, H6 of phenyl ring of pq), 4.68 (s, 2H, CH_2 on C4 of bpy), 3.99 (dd, *J* = 8.8, 2.4 Hz, 1H, H1 of glucose), 3.85−3.81 (m, 3H, H6 of glucose and CH_2O), 3.68−3.59 (m, 11H, H6 of glucose and CH_2O), 3.44 (dt, *J* = 8.8, 2.4 Hz, 1H, H2 of glucose), 3.37 (t, *J* = 8.8 Hz, 1H, H3 of glucose), 3.29−3.26 (dd, 1H, *J* = 8.4, 1.6 Hz, H4 of glucose), 3.24−3.19 (m, 1H, H5 of glucose), 2.69 (s, 3H, CH_3N), 2.46 (s, 3H, CH_3 of bpy). IR (KBr) ν/cm^{-1}: 3420 (O−H), 1073 (C−O), 842 (PF_6^-). MS (ESI$^+$): *m*/*z* 1125 [M − PF_6^-]$^+$. Anal. Calcd for $IrC_{55}H_{57}N_5O_9PF_6{\cdot}4CH_2Cl_2$ (%): C, 44.04; H, 4.07; N, 4.35. Found: C, 43.88; H, 4.30; N, 4.60.

[Ir(pq)$_2$(bpy-TEG-ONCH$_3$-β-D-gal)](PF$_6$) (3b). The synthetic procedure was reported previously.[3] ^{1}H NMR (400 MHz, CD_3OD, 298 K, TMS): δ 8.40−8.39 (m, 4H, H3 of quinoline of pq, H3 and H6 of bpy), 8.25 (s, 1H, H3′ of bpy), 8.19−8.16 (m, 4H, H3 of phenyl ring and H4 of quinoline of pq), 8.08 (d, *J* = 5.6 Hz, 1H, H6′ of bpy), 7.83 (d, *J* = 8.0 Hz, 2H, H8 of quinoline of pq), 7.56 (d, *J* = 5.6 Hz, 1H, H5 of bpy), 7.41−7.37 (m, 5H, H5′ of bpy, H5 and H7 of quinoline of pq), 7.16 (t, *J* = 7.6 Hz, 2H, H4 of phenyl ring of pq), 7.05 (t, *J* = 6.0 Hz, 2H, H6 of quinoline of pq), 6.79 (t, *J* = 7.6 Hz, 2H, H5 of phenyl ring of pq), 6.51 (t, *J* = 7.6 Hz, 2H, H6 of phenyl ring of pq), 4.70 (s, 2H, CH_2 on C4 of bpy), 3.97 (dd, *J* = 9.0, 2.0 Hz, 1H, H1 of galactose), 3.87−3.84 (m, 2H, CH_2O), 3.80 (t, *J* = 3.6 Hz, 1H, H4 of galactose), 3.72−3.46 (m, 15H, H2, H3, H5, H6, of galactose and CH_2O), 2.71 (s, 3H, CH_3N), 2.45 (s, 3H, CH_3 on of bpy). IR (KBr) ν/cm^{-1}: 3422 (O−H), 1094 (C−O), 847 (PF_6^-). MS (ESI$^+$): *m*/*z* 1125 [M − PF_6^-]$^+$. Anal. Calcd for $IrC_{55}H_{57}N_5O_9PF_6{\cdot}5CH_2Cl_2$ (%): C, 42.53; H, 3.99; N, 4.13. Found: C, 42.40; H, 4.19; N, 4.20.

[Ir(bzq)$_2$(bpy-TEG-ONCH$_3$-β-D-glc)](PF$_6$) (4a). The synthetic procedure was similar to that of complex **1a** except that [Ir_2(bzq)$_4Cl_2$] (117.2 mg, 0.10 mmol) was used instead of [Ir_2(bt)$_4Cl_2$]. The complex was isolated as yellow crystals. Yield: 123 mg (50%). ^{1}H NMR (400 MHz, CD_3OD, 298 K, TMS): δ 8.71 (s, 1H, H3 of bpy), 8.63 (s, 1H, H3′ of bpy), 8.43 (d, *J* = 7.0 Hz, 2H, H4 of bzq), 8.05 (t, *J* = 5.2 Hz, 2H, H2 of bzq), 7.93−7.90 (m, 3H, H6 of bpy and H6 of bzq), 7.80−7.77 (m, 3H, H6′ of bpy and H5 of bzq), 7.52−7.49 (m, 4H, H3 and H7 of bzq), 7.44 (d, *J* = 5.2 Hz, 1H, H5 of bpy), 7.27 (d, *J* = 5.6 Hz, 1H, H5′ of bpy), 7.14 (dt, *J* = 7.8, 2.8 Hz, 2H, H8 of bzq), 6.32−6.29 (m, 2H, H9 of bzq), 4.80 (s, 2H, CH_2 on C4 of bpy), 3.97 (dd, *J* = 8.8, 3.2 Hz, 1H, H1 of glucose), 3.83−3.58 (m, 14H, H6 of glucose and CH_2O), 3.47−3.35 (m, 2H, H2 and H3 of glucose), 3.27−3.20 (m, 2H, H4 and H5 of glucose), 2.67 (s, 3H, CH_3N), 2.57 (s, 3H, CH_3 of bpy). IR (KBr) ν/cm^{-1}: 3448 (O−H), 846 (PF_6^-). MS (ESI$^+$): *m*/*z* 1073 [M − PF_6^-]$^+$. Anal. Calcd for $IrC_{51}H_{53}N_5O_9PF_6{\cdot}2H_2O{\cdot}CH_2Cl_2$ (%): C, 46.67; H, 4.44; N, 5.23. Found: C, 46.90; H, 4.66; N, 5.29.

[Ir(bzq)$_2$(bpy-TEG-ONCH$_3$-β-D-gal)](PF$_6$) (4b). The synthetic procedure was similar to that of complex **1b** except that [Ir_2(bzq)$_4Cl_2$] (115.4 mg, 98.8 μmol) was used instead of [Ir_2(bt)$_4Cl_2$]. The complex was isolated as light brown crystals. Yield: 192 mg (96%). ^{1}H NMR (400 MHz, CD_3OD, 298 K, TMS): δ 8.72 (s, 1H, H3 of bpy), 8.63 (s, 1H, H3′ of bpy), 8.43 (d, *J* = 8.0 Hz, 2H, H4 of bzq), 8.05 (t, *J* = 5.2 Hz, 2H, H2 of bzq), 7.92−7.89 (m, 3H, H6 of bpy and H6 of bzq), 7.80−7.77 (m, 3H, H6′ of bpy and H5 of bzq), 7.52−7.49 (m, 4H, H3,

dx.doi.org/10.1021/ic401714p | Inorg. Chem. 2013, 52, 13029−13041

H7 of bzq), 7.44 (d, J = 5.6 Hz, 1H, H5 of bpy), 7.26 (d, J = 5.2 Hz, 1H, H5′ of bpy), 7.14 (dt, J = 7.6, 2.4 Hz, 2H, H8 of bzq), 6.31−6.28 (m, 2H, H9 of bzq), 4.79 (s, 2H, CH_2 on C4 of bpy), 3.96 (dd, J = 9.2, 4.8 Hz, 1H, H1 of galactose), 3.81−3.44 (m, 18 H, CH_2O and H2, H3, H4, H5, H6 of galactose), 2.66 (d, J = 4.8 Hz, 3H, CH_3N), 2.57 (s, 3H, CH_3 of bpy). IR (KBr) ν/cm^{-1}: 3421 (O−H), 844 (PF_6^-). MS (ESI$^+$): m/z 1073 [M − PF_6^-]$^+$. Anal. Calcd for $IrC_{51}H_{53}N_5O_9PF_6{\cdot}1.5CH_3COCH_3$ (%): C, 51.11; H, 4.79; N, 5.37. Found: 51.41; H, 4.55; N, 5.61.

Physical Measurements and Instrumentation. The instrumentation for physical measurements has been described previously.[13] Briefly, ^{1}H NMR spectra were recorded on a Varian Mercury 300 MHz or a Bruker 400 MHz NMR spectrometer at 298 K. Positive-ion electrospray ionization (ESI) mass spectra were recorded on a Perkin-Elmer Sciex API 365 mass spectrometer. IR spectra of the samples in KBr pellets were recorded in the range 4000−400 cm^{-1} using a Perkin-Elmer FTIR-1600 spectrophotometer. Elemental analyses were carried out on an Elementar Analysensysteme GmbH Vario MICRO elemental analyzer. Electronic absorption and steady-state emission spectra were recorded on a Hewlett-Packard 8453 diode array spectrophotometer and a SPEX FluoroLog 3-TCSPC spectrophotometer, respectively. Emission lifetimes were measured in the Fast MCS or TCSPC mode with a NanoLED N-375 as the excitation source. Unless specified, all the solutions for photophysical studies were degassed with no fewer than four successive freeze−pump−thaw cycles, stored in a 10 cm^3 round-bottomed flask equipped with a side arm 1-cm fluorescence cuvette, and sealed from the atmosphere by a Rotaflo HP6/6 quick-release Teflon stopper. Luminescence quantum yields were measured by the optically dilute method[14] with an aerated aqueous solution of $[Ru(bpy)_3]Cl_2$ (Φ_{em} = 0.028) as the standard solution.[15] The lipophilicity of the complexes was determined from the log k'_w values (k'_w = chromatographic capacity factor at 100% aqueous solution), which were measured by reversed-phase HPLC on a C-18 column according to the method described by Minick.[16]

Cell Cultures. HeLa, HepG2, MCF-7, MDA-MB-231, HEK293T, NIH/3T3, and 3T3-L1 cells were cultured in high glucose DMEM supplemented with 10% FBS and 1% penicillin-streptomycin in a humidified chamber at 37 °C under a 5% CO_2 atmosphere. They were subcultured every 2 to 3 days. Differentiation of the preadipocytes 3T3-L1 was induced by treating postconfluent cells with growth medium containing dexamethasone (1 μM), IBMX (0.5 mM), and insulin (1.0 μg mL^{-1}) for 48 h. The cells were fed with growth medium containing insulin (1.0 μg mL^{-1}) every other day for the following 7−15 days.

ICP-MS. Cells grown in a 60-mm tissue culture dish were incubated with the iridium(III) complexes (50 μM) in glucose-free medium/DMSO (99:1, v/v) at 37 °C under a 5% CO_2 atmosphere for 5 min. The medium was removed, and the cell layer was washed gently with PBS (1 mL × 3). The cells were then trypsinized and harvested with PBS (500 μL × 4) before being digested with 65% HNO_3 (2 mL) at 70 °C for 2 h. The digested solution was analyzed using an Elan 6100 DRC-ICP-MS (PerkinElmer SCIEX Instruments).

MTT Assays. Cells were seeded in a 96-well flat-bottomed microplate (*ca.* 10 000 cells per well) in growth medium (100 μL) and incubated at 37 °C under a 5% CO_2 atmosphere for 24 h. The iridium(III) complexes and cisplatin (positive control), respectively, in different concentrations, were added to the wells in a mixture of growth medium/DMSO (99:1, v/v). After the microplate was incubated for 48 h, MTT in PBS (5 mg mL^{-1}, 10 μL) was added to each well. The microplate was then incubated for another 4 h. The medium was removed carefully, and isopropanol (200 μL) was added to each well. The microplate was further incubated for 5 min. The absorbance of the solutions at 570 nm was measured with a SPECTRAmax 340 microplate reader (Molecular Devices Corp., Sunnyvale, CA). The IC_{50} values of the complexes were determined from dose dependence of surviving cells after exposure to the iridium(III) complexes and cisplatin.

Live-Cell Confocal Imaging. Cells in growth medium were seeded on a sterilized coverslip in a 60-mm tissue culture dish and grown at 37 °C under a 5% CO_2 atmosphere for 48 h. The growth medium was removed and replaced with glucose-free medium/DMSO (99:1, v/v) containing the iridium(III) complexes (50 μM). After incubation for 5 min, the medium was removed, and the cell layer was washed gently with PBS (1 mL × 3). The coverslip was mounted onto a sterilized glass slide and then imaged using a Leica TCS SPE confocal microscope with an oil immersion 40× or 63× objective and an excitation wavelength at 405 nm. The emission was measured using a long-pass filter at 532 nm. The excitation wavelength for imaging experiments involving MitoTracker Deep Red FM was 633 nm. The Pearson's Coefficient was determined by the program Image J. The excitation wavelength was 488 nm for the photostability experiments involving complex **1a** and 2-NBDG.

Hexokinase Assays. The iridium(III) bipyridine complexes (0.5 mM, 10 μL) in DMSO were added to a reaction vial which contained hexokinase (3.76 U), ATP (1 mM), and $MgCl_2$ (4 mM) in a Tris-Cl buffer (30 mM, pH 6.0) to give a final volume of 1 mL. The resulting solutions were mixed gently by inversion, and allowed to incubate for 24 h at 37 °C in the dark. Each solution (100 μL) was extracted with CH_2Cl_2 (100 μL × 3). The combined organic layer with or without the presence of 0.1% acetic acid was analyzed by ESI-MS.

RESULTS AND DISCUSSION

Synthesis. There is a growing interest in using the *N*-methylamino-oxy group to functionalize unprotected reducing sugars as it reacts readily with the sugars at the reducing end under mild conditions, and the derivatized sugars are primarily in the closed-chain form. In this work, the bipyridine-sugar ligands were obtained from the reaction of 4-(10-*N*-methylamino-oxy-2,5,8-trioxa-dec-1-yl)-4′-methyl-2,2′-bipyridine (bpy-TEG-ONHCH$_3$) with D-glucose or D-galactose under mildly acidic conditions. The sugar-free bipyridine ligand bpy-TEG-OMe was synthesized from the reaction of 4-(10-hydroxy-2,5,8-trioxa-dec-1-yl)-4′-methyl-2,2′-bipyridine (bpy-TEG-OH)[10c] with CH_3I in DMF in the presence of sodium hydride. The iridium(III) complexes were prepared from the reaction of $[Ir_2(N^\wedge C)_4Cl_2]$ (HN^C = Hbt, Hppy, Hpq, Hbzq) with the bipyridine derivatives in CH_2Cl_2 or a mixture of CH_2Cl_2/MeOH (1:1, v/v), which was followed by anion exchange with KPF_6. Subsequent recrystallization from CH_2Cl_2/diethyl ether afforded the complexes as yellow or orange crystals. The complexes were characterized by ^{1}H NMR spectroscopy, positive-ion ESI-MS, and IR spectroscopy and gave satisfactory elemental analyses.

Photophysical Properties. The electronic absorption spectral data of the iridium(III) complexes in CH_2Cl_2 and CH_3CN at 298 K are listed in Table 1. The electronic absorption spectra of the glucose complexes **1a**−**4a** in CH_2Cl_2 at 298 K are shown in Figure 1. All the iridium(III) complexes showed intense spin-allowed intraligand (^{1}IL) ($\pi \rightarrow \pi^*$) (N^C and N^N) absorption features in the UV region (*ca.* 253 − 412 nm, ε on the order of 10^4 dm^3 mol^{-1} cm^{-1}) and weaker spin-allowed metal-to-ligand charge-transfer (^{1}MLCT) [dπ(Ir) → π^*(N^N and N^C)] absorption shoulders or bands in the visible region (>*ca.* 415 nm). The weaker absorption tailing beyond *ca.* 470 nm has been assigned to spin-forbidden ^{3}MLCT [dπ(Ir) → π^*(N^N and N^C)] transitions.[10−12]

Photoexcitation of the complexes resulted in intense and long-lived green to yellow emission in fluid solutions under ambient conditions and in low-temperature alcohol glass (Table 2). The emission spectra of the glucose complexes **1a**−**4a** in CH_2Cl_2 at 298 K are shown in Figure 2. The bt (**1a**−**1c**) and pq (**3a** and **3b**) complexes displayed vibronically structured emission features and very long emission lifetimes (τ_o > 2 μs) in fluid solutions at 298 K (Table 2). Also, the emission properties of these complexes were not very sensitive to the polarity of the solvents, suggestive of a ^{3}IL ($\pi \rightarrow \pi^*$) (bt/pq) emissive state.[10−12,17,18] In contrast, the ppy (**2a** and **2b**) and bzq (**4a** and **4b**) complexes showed a broad emission

dx.doi.org/10.1021/ic401714p | Inorg. Chem. 2013, 52, 13029−13041

Table 1. Electronic Absorption Spectral Data of the Iridium(III) Complexes at 298 K

complex	solvent	λ_{abs} (nm) (ε (dm^3 mol^{-1} cm^{-1}))
1a	CH_2Cl_2	259 sh (50 690), 270 (49 215), 291 sh (43 930), 310 (49 895), 323 (45 685), 378 sh (12 300), 412 (10 435), 444 sh (7450)
	CH_3CN	256 sh (37 690), 267 (35 880), 294 sh (32 445), 308 (35 630), 322 (32 780), 376 sh (8655), 411 (7255), 443 sh (4960)
	buffer[a]	255 sh (36 155), 267 (34 090), 294 sh (30 860), 309 (34 300), 321 (31 520), 378 sh (8290), 411 (7080), 455 sh (4475)
1b	CH_2Cl_2	260 sh (41 580), 275 sh (39 230), 295 sh (36 625), 311 (41 285), 323 (38 440), 379 sh (10 085), 411 (8700), 441 sh (7050)
	CH_3CN	255 sh (37 075), 272 sh (34 230), 293 sh (31 075), 309 (35 395), 322 (32 855), 379 sh (7810), 412 (7115), 433 sh (6010)
	buffer[a]	255 sh (32 750), 267 (30 940), 295 sh (28 020), 309 (31 235), 321 (28 805), 378 sh (7455), 411 (6440), 442 sh (4465)
1c	CH_2Cl_2	258 sh (40 050), 270 (38 760), 291 sh (34 550), 310 (37 950), 323 (34 660), 354 sh (13 120), 377 sh (9525), 412 (7850), 440 sh (6240)
	CH_3CN	253 sh (33 220), 270 sh (31 455), 295 sh (29 035), 308 (31 290), 324 (27 885), 351 sh (11 910), 374 sh (8445), 412 (6725), 438 sh (5215)
	buffer[a]	255 sh (44 030), 267 (41 535), 293 sh (37 495), 309 (41 725), 321 (38 330), 379 sh (9610), 410 (8395), 444 sh (5375)
2a	CH_2Cl_2	258 (48 815), 269 sh (45 755), 277 sh (40 310), 313 sh (20 345), 340 sh (9940), 386 sh (5810), 417 sh (3555)
	CH_3CN	256 (44 160), 277 sh (31 495), 312 sh (17 300), 344 sh (8125), 381 sh (5035), 417 sh (2975)
	buffer[a]	256 sh (53 300), 271 sh (46 480), 280 sh (36 465), 314 sh (18 540), 347 sh (8965), 385 sh (5630), 425 sh (2405)
2b	CH_2Cl_2	258 (46 290), 270 sh (43 150), 278 sh (37 425), 314 sh (18 230), 343 sh (8910), 385 sh (5730), 415 sh (3545)
	CH_3CN	255 (48 660), 276 sh (36 125), 312 sh (18 655), 345 sh (8545), 384 sh (5210), 419 sh (2980)
	buffer[a]	256 sh (62 400), 271 sh (54 405), 279 sh (44 230), 311 sh (25 595), 345 sh (10 930), 385 sh (6660), 420 sh (3460)
3a	CH_2Cl_2	264 sh (54 410), 273 (55 905), 283 sh (53 910), 311 sh (23 750), 338 (24 955), 350 sh (22 710), 443 (5335)
	CH_3CN	262 sh (49 535), 270 (50 175), 280 sh (47 615), 309 sh (21 920), 336 (22 290), 351 sh (18 865), 440 (4985)
	buffer[a]	262 sh (59 545), 270 (60 665), 285 sh (51 225), 310 sh (26 365), 337 (26 870), 353 sh (21 600), 435 (5960)
3b	CH_2Cl_2	263 sh (50 875), 274 (52 785), 283 sh (51 465), 310 sh (23 845), 337 (24 110), 355 sh (18 995), 442 (5460)
	CH_3CN	262 sh (44 130), 273 (44 600), 281 sh (41 835), 309 sh (20 230), 336 (20 045), 352 sh (16 595), 439 (4065)
	buffer[a]	263 sh (39 460), 270 (40 120), 285 sh (33 705), 310 sh (17 085), 337 (17 830), 353 sh (14 270), 435 (3960)
4a	CH_2Cl_2	255 (50 570), 290 sh (23 610), 311 (20 030), 340 sh (14 595), 419 (4845)
	CH_3CN	262 sh (44 170), 288 sh (22 205), 309 (21 550), 335 sh (15 790), 416 (4750)
	buffer[a]	261 sh (52 340), 292 sh (26 335), 309 (34 695), 341 sh (16 040), 429 sh (4205)
4b	CH_2Cl_2	266 sh (50 265), 293 sh (28 600), 310 (24 495), 355 sh (13 720), 429 (5050)
	CH_3CN	263 sh (43 685), 291 sh (22 580), 309 (20 115), 342 sh (13 865), 430 sh (3790)
	buffer[a]	260 sh (47 070), 289 sh (24 075), 308 (21 065), 341 sh (13 990), 429 sh (3875)

[a]50 mM potassium phosphate buffer pH 7.4/MeOH (7:3, v/v).

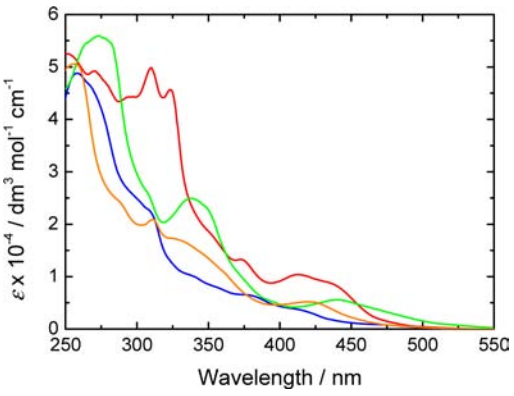

Figure 1. Electronic absorption spectra of complexes **1a** (red), **2a** (blue), **3a** (green), and **4a** (orange) in CH_2Cl_2 at 298 K.

band with positive solvatochromism in fluid solutions at 298 K, which indicated that the emission originated from a ^{3}MLCT [dπ(Ir) → π^*(N^N)] excited state.[10,17] This is supported by the observation of significant blue-shifts of their emission maxima upon cooling the samples from 298 to 77 K, which was not exhibited by the bt and pq complexes. On the basis of the photophysical data (Table 2), it appears that the sugar pendants did not significantly perturb the photophysical properties of the complexes.

Lipophilicity, Cellular Uptake Efficiency, and Cytotoxic Activity. The lipophilicity of the complexes has been determined by reversed-phase HPLC, and the log $P_{o/w}$ values are listed in Table 3. The lipophilicity of the iridium(III) complexes (log $P_{o/w}$ ranged from 1.40 to 2.59) was significantly higher than that of cisplatin (−2.30). The bt (**1a**−**1c**), pq (**3a** and **3b**), and bzq (**4a** and **4b**) complexes showed substantially higher lipophilicity compared with their ppy (**2a** and **2b**) counterparts, which is a consequence of the additional hydrophobic phenyl rings of their cyclometalating ligands.[17c,d,20] As expected, we did not observe significantly different lipophilicity between the D-glucose and D-galactose complexes with the same cyclometalating ligands. However, the log $P_{o/w}$ values of the D-glucose (**1a**) (log $P_{o/w}$ = 2.44) and D-galactose (**1b**) (log $P_{o/w}$ = 2.30) complexes were slightly smaller than that of their sugar-free counterpart complex **1c** (log $P_{o/w}$ = 2.59), illustrating the effect of the polar sugar entity in reducing the overall lipophilicity of the complexes.

The cellular uptake of the complexes by human cervix epithelioid carcinoma cells (HeLa) has been determined by ICP-MS experiments. The results showed that an average HeLa cell incubated with the complexes (50 μM) at 37 °C for 5 min contained 0.21−5.43 fmol of iridium (Table 3), which is comparable to other cyclometalated iridium(III) polypyridine complexes.[10b−e,g,13,20b] In general, the ability of a compound to permeate cell membrane is strongly dependent on its lipophilicity, especially if the uptake pathway is passive diffusion in nature.[21] This explains the higher uptake of complex **1c** compared with its less lipophilic sugar counterparts, complexes **1a** and **1b**. Interestingly, although the lipophilicity of the D-glucose and D-galactose was similar, there was noticeable difference in the uptake efficiency between the complexes appended with these sugars; for example, the D-glucose complexes of bt (**1a**) and pq (**3a**) showed higher intracellular iridium than their D-galactose counterparts [the bt (**1b**) and pq (**3b**) complexes], while the reverse was observed for the ppy (**2a** and **2b**) and bzq (**4a** and **4b**) pairs. The reasons for these

dx.doi.org/10.1021/ic401714p | Inorg. Chem. 2013, 52, 13029−13041

Table 2. Photophysical Data of the Iridium(III) Complexes

complex	medium (T (K))	λ_{em} (nm)	τ_o (μs)	Φ_{em}
1a	CH_2Cl_2 (298)	521 (max), 559, 606 sh, 669 sh	3.78	0.59
	CH_3CN (298)	524 (max), 561, 612 sh, 670 sh	3.77	0.58
	buffer (298)[a]	523 (max), 561, 612 sh, 669 sh	3.04	0.48
	glass (77)[b]	515 (max), 533 sh, 557, 576 sh, 604, 630 sh	5.02	
1b	CH_2Cl_2 (298)	522 (max), 560, 615 sh, 670 sh	3.87	0.57
	CH_3CN (298)	525 (max), 562, 620 sh, 680 sh	3.83	0.51
	buffer (298)[a]	524 (max), 560, 615 sh, 670 sh	3.02	0.40
	glass (77)[b]	514 (max), 532 sh, 556, 576 sh, 603, 628 sh	5.03	
1c	CH_2Cl_2 (298)	521 (max), 559, 610 sh, 669 sh	3.86	0.76
	CH_3CN (298)	524 (max), 561, 612 sh, 670 sh	3.75	0.55
	buffer (298)[a]	524 (max), 561, 612 sh, 669 sh	3.01	0.43
	glass (77)[b]	515 (max), 531 sh, 557, 576 sh, 605, 630 sh	5.06	
2a	CH_2Cl_2 (298)	568	0.64	0.29
	CH_3CN (298)	577	0.38	0.13
	buffer (298)[a]	588	0.098	0.025
	glass (77)[b]	472, 511 (max), 535 sh	4.77	
2b	CH_2Cl_2 (298)	570	0.63	0.28
	CH_3CN (298)	576	0.38	0.14
	buffer (298)[a]	584	0.11	0.022
	glass (77)[b]	472, 501 (max), 532 sh	4.90	
3a	CH_2Cl_2 (298)[c]	554, 588 sh	2.62	0.72
	CH_3CN (298)[c]	557	2.82	0.73
	buffer (298)[a]	556	2.24	0.45
	glass (77)[b,c]	539 (max)	4.71	
3b	CH_2Cl_2 (298)[c]	554, 589 sh	2.67	0.80
	CH_3CN (298)[c]	557	2.86	0.84
	buffer (298)[a]	556	2.21	0.45
	glass (77)[b,c]	540 (max)	4.69	
4a	CH_2Cl_2 (298)	575	0.63	0.24
	CH_3CN (298)	578	0.36	0.10
	buffer (298)[a]	587	0.074	0.021
	glass (77)[b]	499 (max), 538, 584 sh, 639 sh	57.8 (90%), 110.1 (10%)	
4b	CH_2Cl_2 (298)	571	0.60	0.16
	CH_3CN (298)	576	0.37	0.08
	buffer (298)[a]	589	0.076	0.017
	glass (77)[b]	501 (max), 535, 589 sh	49.8 (81%), 102.2 (19%)	

[a]50 mM potassium phosphate buffer pH 7.4/MeOH (7:3, v/v). [b]EtOH/MeOH (4:1, v/v). [c]From ref 10c.

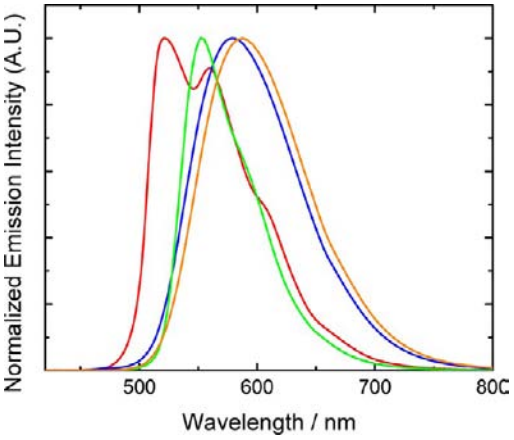

Figure 2. Emission spectra of complexes **1a** (red), **2a** (blue), **3a** (green), and **4a** (orange) in CH_2Cl_2 at 298 K.

Table 3. Lipophilicity, Cellular Uptake, and IC_{50} Values of the Iridium(III) Complexes and Cisplatin

complex	log $P_{o/w}$	amount of complex[a] (fmol)	IC_{50}[b] (μM)
1a	2.44	4.02 ± 0.05	1.40 ± 0.07
1b	2.30	1.03 ± 0.15	5.87 ± 1.81
1c	2.59	5.43 ± 0.57	0.10 ± 0.02
2a	1.46	0.21 ± 0.04	>230
2b	1.40	0.52 ± 0.02	1.80 ± 0.18
3a	2.56	0.95 ± 0.01	4.00 ± 0.60[c]
3b	2.53	0.40 ± 0.005	12.0 ± 1.30[c]
4a	2.48	0.79 ± 0.04	29.6 ± 6.94
4b	2.37	2.07 ± 0.23	7.06 ± 1.09
cisplatin	−2.30[d]	N.A.	22.3 ± 0.77

[a]Amount of iridium associated with an average HeLa cell upon incubation with the complexes (50 μM) in a glucose-free medium at 37 °C for 5 min as determined by ICP-MS. [b]HeLa cells, incubated in high glucose DMEM for 48 h. [c]From ref 10c. [d]From ref 19.

observations are unknown at this stage. However, as it has been documented that the uptake of D-glucose and D-galactose is facilitated by different GLUTs,[1d,e,22,23] we believe that the different degrees of uptake of the complexes should be due to a combined effect of energy-dependent internalization/externalization (e.g., endocytosis and probably SGLTs)[1e,22a] and GLUT-mediated transport (see below). Thus, we have confined the scope of this study in the possible role of GLUTs on the cellular uptake of the D-glucose complexes.

The cytotoxic activity of the complexes toward HeLa cells for an incubation period of 48 h has been evaluated by the MTT assay.[24] The IC_{50} values were in the micromolar scale (Table 3), and almost all of them were smaller than that of cisplatin (22.3 μM) under the same experimental conditions. These values are comparable to those of other cyclometalated iridium(III) polypyridine complexes.[10a,c,e,g,13,17d,20,25] As expected, there was strong dependence of the cytotoxicity of the complexes on their cellular uptake. In particular, the ppy−glucose complex **2a**, which showed the least efficient uptake (0.21 fmol), had the highest IC_{50} value (>230 μM). In contrast, the most lipophilic sugar-free complex **1c**, which showed the highest uptake efficiency, was the most cytotoxic among the complexes in this study. It is likely that the cytotoxicity of the complexes originates from their localization and effects on specific organelles such as mitochondria (see below).[10f,26]

Uptake Mechanism and Inhibition Studies. The possible involvement of GLUTs in the cellular uptake properties of the bt−glucose (**1a**) and bt−galactose (**1b**) complexes has been further investigated because their uptake efficiency was very different (Table 3). Treatment of HeLa cells with these complexes (50 μM) in a glucose-free medium at 4 °C resulted in a reduction of intracellular iridium uptake by *ca.*

dx.doi.org/10.1021/ic401714p | Inorg. Chem. 2013, 52, 13029−13041

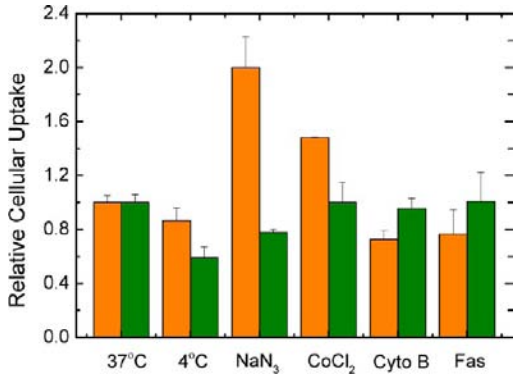

Figure 3. Relative cellular uptake of iridium associated with an average HeLa cell upon incubation with complexes **1a** (orange) and **1b** (green) (50 μM) at 37 °C (respective reference points) and 4 °C for 5 min and after preincubation with NaN_3 (3 mM, 30 min), $CoCl_2$ (250 μM, 2 h), cytochalasin B (10 μM, 1 h), and fasentin (80 μM, 1 h), respectively.

20% and 40%, respectively (Figure 3). This indicates that (1) both complexes entered the cells, to a certain extent, by an energy-dependent pathway, and (2) this pathway appears to be less important to the glucose complex **1a**. When the cells were pretreated with the oxidative phosphorylation inhibitor sodium azide[27] (3 mM) for 30 min, a decrease of intracellular iridium (*ca.* 20% with respect to untreated cells) was observed for the cells loaded with the galactose complex **1b** (Figure 3). This is expected because of the cellular energy depletion caused by the reagent. In sharp contrast, addition of sodium azide led to an *increase* of intracellular iridium by about 2-fold in the cells incubated with the glucose complex **1a**. Since exposure of cells to azide results in a decline in cellular ATP content due to immediate inhibition of oxidative phosphorylation, glucose transport is rapidly stimulated as a consequence.[28] Thus, the increased uptake strongly suggested that complex **1a** was internalized through a GLUT-dependent pathway. Upon exposure of the cells to a GLUT-upregulating reagent cobalt(II) chloride[28b,29] (250 μM) for 2 h, the glucose complex **1a** exhibited an increased uptake efficiency (Figure 3). However, the reverse was observed when the cells were treated with GLUT1 inhibitors cytochalasin B[30] (10 μM) and fasentin[31] (80 μM), respectively, for 1 h prior to complex incubation. On the contrary, uptake of the galactose complex **1b** by HeLa cells was not affected by any of these reagents and biomolecules. To sum up, all these results indicated that GLUTs play a very important role in the uptake of complex **1a** by HeLa cells.

Effects of Glucose on Uptake. It has been well documented that for any glucose derivatives entering cells through a GLUT-mediated pathway, their uptake is competitively inhibited by D-glucose and 2-deoxy-D-glucose but independent of L-glucose (Scheme 1).[6b,d,e,7c−e,32] In this work, the effects of D-glucose on the cellular uptake properties of complexes **1a** and **1b** have been investigated. Incubation of HeLa cells with the glucose complex **1a** (50 μM) at 37 °C for 5 min in the presence of 50 mM D-glucose in a glucose-free medium resulted in reduced emission intensity of the HeLa cells (Figure 4). In contrast, cells treated with the galactose complex **1b** did not show any significant changes in emission intensity in the presence of D-glucose (Figure S1, Supporting Information). ICP-MS measurements also revealed the inhibitory effect of D-glucose to the uptake of complex **1a**. Upon incubation of HeLa cells with complex **1a** (50 μM, 5 min)

Scheme 1. Schematic Representation of GLUT-Mediated Uptake of Luminescent Glucose Derivatives

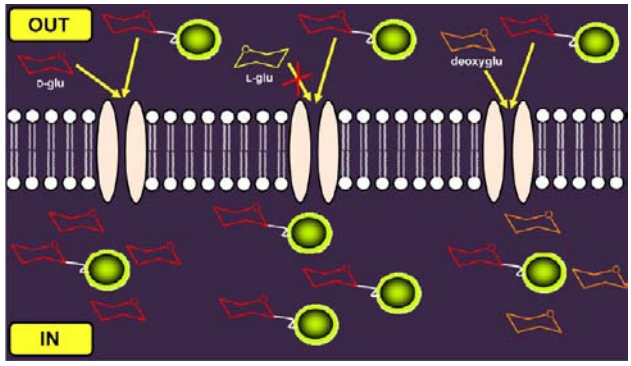

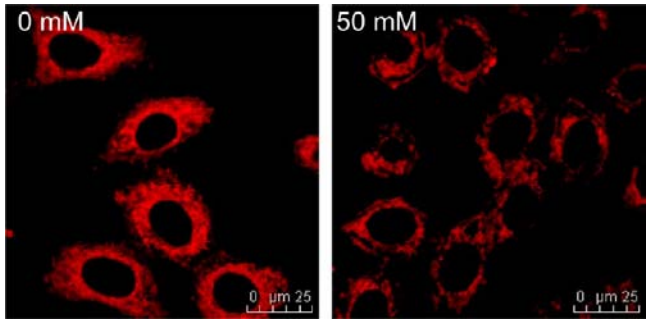

Figure 4. Laser-scanning confocal microscopy images of HeLa cells upon incubation with complex **1a** (50 μM) in a glucose-free medium containing 0 mM (left) and 50 mM (right) of D-glucose at 37 °C for 5 min, respectively.

in the presence of 0−50 mM of D-glucose or L-glucose in a glucose-free medium, only D-glucose, but not L-glucose, decreased the intracellular concentration of the complex by *ca.* 40% (Figure 5, top and middle, orange bars). Additionally, the presence of increasing amounts of 2-deoxy-D-glucose in the medium resulted in a similar reduction of cellular uptake of complex **1a** (Figure 5, bottom, orange bars). On the contrary, the uptake of the galactose complex **1b** by HeLa cells did not exhibit any similar changes under the same conditions (Figure 5, green bars). All these findings support that the glucose moiety of complex **1a** renders it to be internalized through a GLUT-dependent pathway.

Cell Line Dependence. In order to support high metabolic functions, cancer cells usually show enhanced glucose uptake and glycolytic rates compared to nontumorigenic cells. This feature has been frequently correlated to the elevated expression of GLUTs and hexokinase.[6d,33] Thus, cellular probes that show GLUT-mediated uptake can be reflected by more efficient internalization toward transformed cell lines than nontransformed cells (Scheme 2). The uptake of complexes **1a** and **1b** by two transformed cell lines, HeLa and human breast adenocarcinoma (MCF-7), and two nontransformed cell lines, human embryonic kidney cells (HEK293T) and mouse embryonic fibroblasts (NIH/3T3), has been investigated, and the data are summarized in Table 4. Interestingly, the intracellular amounts of iridium in HeLa and MCF-7 cells incubated with the glucose complex **1a** were considerably larger than those in HEK293T and NIH/3T3 cells. However, no trend was observed for the cells incubated with the galactose complex **1b**. These results further highlight the important role of GLUTs on the uptake of the glucose complex. In accordance

dx.doi.org/10.1021/ic401714p | *Inorg. Chem.* 2013, 52, 13029−13041

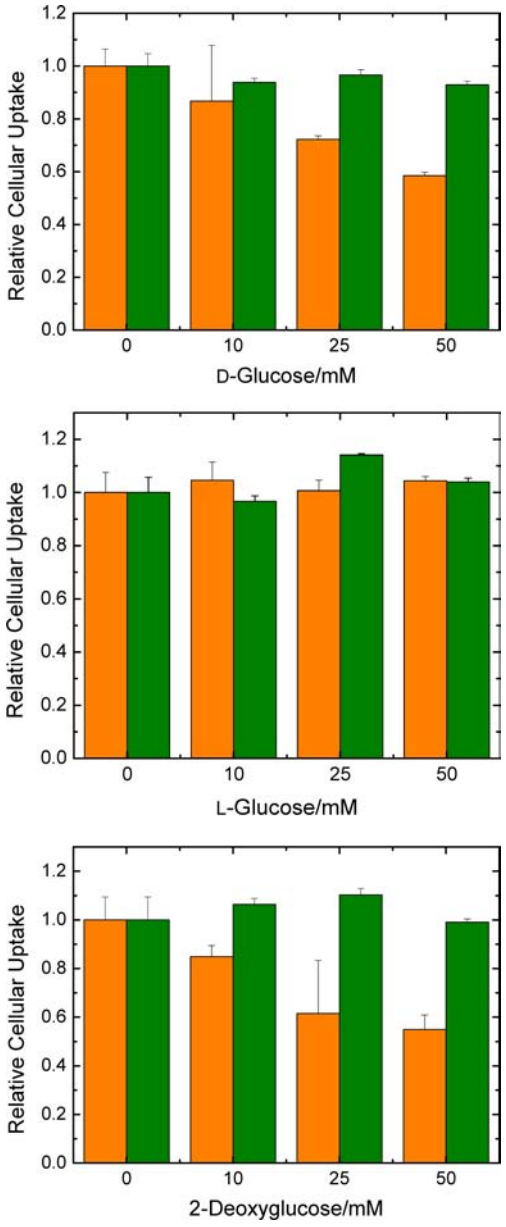

Figure 5. Relative cellular uptake of iridium associated with an average HeLa cell upon incubation with complexes **1a** (orange) and **1b** (green) (50 μM) at 37 °C for 5 min in a glucose-free medium containing various concentration of D-glucose (top), L-glucose (middle), and 2-deoxyglucose (bottom). The uptake of complexes **1a** and **1b** in the absence of sugar was set as respective reference points.

with the different cellular uptake efficiency toward these cell lines, MTT assays revealed that complex **1a** was more cytotoxic toward the transformed cell lines compared to the non-transformed ones, and no similar dependence was observed for its galactose counterpart complex **1b** (Table 4).

Hexokinase Assays. In the first step of glucose metabolism, hexokinase catalyzes the transfer of a phosphate group from ATP to the hydroxyl group at the C6 position of glucose. This phosphorylation assists in trapping of glucose for further cellular manipulations. To examine the possible interaction of our iridium(III) glucose complexes with hexokinase, *in vitro* assays mimicking the phosphorylation reaction have been performed.[6c] As expected, we did not

Scheme 2. Schematic Representation of Cellular Internalization of Luminescent Glucose Derivatives toward Transformed and Nontransformed Cells

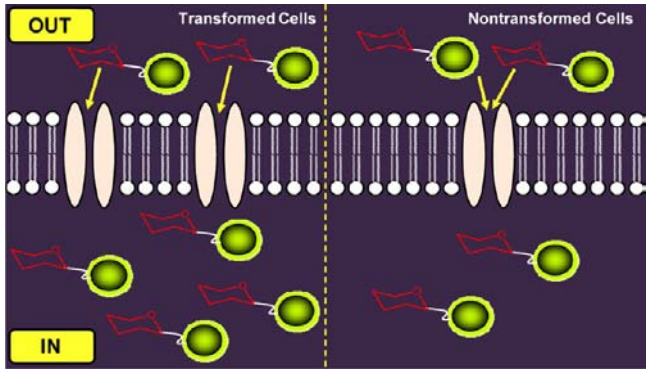

Table 4. Cellular Uptake and IC_{50} Values of the Iridium(III) Complexes toward Different Cell Lines

	amount of complex[a] (fmol)		IC_{50}[b] (μM)	
cell line	**1a**	**1b**	**1a**	**1b**
HeLa	3.76 ± 0.21	0.90 ± 0.02	1.40 ± 0.07	5.87 ± 1.81
MCF-7	2.49 ± 0.12	1.43 ± 0.01	3.55 ± 0.61	3.76 ± 1.06
HEK293T	0.39 ± 0.03	0.77 ± 0.15	6.12 ± 1.28	3.20 ± 0.28
NIH/3T3	1.11 ± 0.11	1.51 ± 0.12	10.4 ± 0.48	7.58 ± 0.35

[a][Ir] = (50 μM), incubation in glucose-free DMEM at 37 °C for 5 min. [b]Incubation in high glucose DMEM for 48 h.

observe any phosphorylation of the galactose complexes **1b**−**4b** from the ESI-MS analyses.[34] Similarly, the glucose complexes **1a**−**4a** did not show phosphorylation either under the same experimental conditions. With reference to similar findings in related systems,[8d−g] it is likely that the extremely rigid structure requirement of the enzyme for its substrates hindered binding and phosphorylation of the glucose complexes.[35]

Effects of Insulin. After confirming the GLUT-mediated uptake of the glucose complex **1a**, we have examined the possibility of using this complex as a glucose uptake indicator for cells in response to different hormonal and metabolic stimulation and inhibition (Scheme 3). Insulin not only

Scheme 3. Schematic Representation of Cellular Internalization of Luminescent Glucose Derivatives upon Hormonal Stimulation and Inhibition

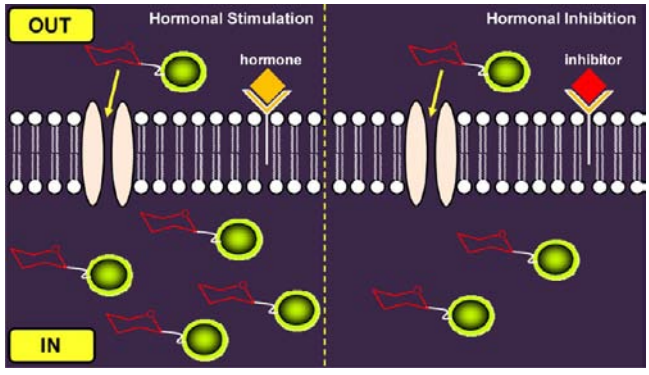

enhances glucose transport and increases glycolytic enzyme activity in normal human cells,[36] but also plays an important role in the stimulation of glucose uptake in cancer cells.[36d,37]

dx.doi.org/10.1021/ic401714p | *Inorg. Chem.* 2013, 52, 13029−13041

The effects of insulin on the cellular uptake of the glucose complex **1a** have been investigated and compared with the galactose and sugar-free complexes **1b** and **1c**, respectively. HeLa cells were treated with complex **1a**, **1b**, or **1c** (50 μM, 5 min) after preincubation with insulin (100 nM, 1 h) in a glucose-free medium. Upon stimulation by the hormone, the intracellular amount of complex **1a** was significantly enhanced by *ca.* 2.7-fold (Figure 6). In contrast, the presence of insulin only caused modest

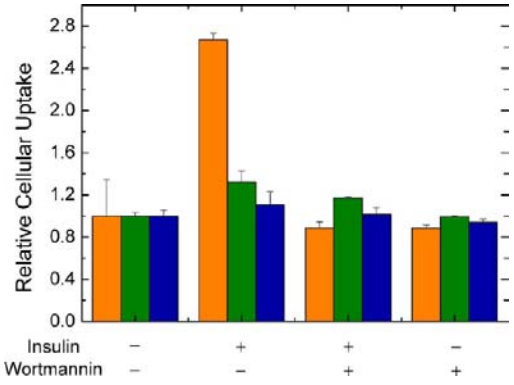

Figure 6. Relative cellular uptake of iridium associated with an average HeLa cell upon incubation with complexes **1a** (orange), **1b** (green), and **1c** (blue) (50 μM) at 37 °C for 5 min with or without preincubation with insulin (100 nM) and wortmannin (1 μM) for 1 h. The uptake of complexes **1a**−**1c** in the absence of insulin and wortmannin was set as respective reference points.

to negligible changes to the uptake of complexes **1b** and **1c**.[38] Interestingly, when the cells were pretreated with an insulin-desensitizer wortmannin (1 μM, 1 h),[6e,39] the stimulation effect of the hormone on the cellular uptake of complex **1a** disappeared. Also, wortmannin alone did not have any effect on the uptake of the complex. It is important to note that the galactose and sugar-free complexes **1b** and **1c** did not show any significant changes in their cellular uptake behavior under the same conditions (Figure 6). Thus, these experiments have established that the GLUT-dependent cellular uptake of complex **1a** responded to external hormonal stimulation and inhibition. Next, we were interested in the possible use of complex **1a** to pursue the insulin-induced cellular translocation of GLUT4 by laser-scanning confocal microscopy.[3e] As shown in Figure 7, complex **1a** was efficiently

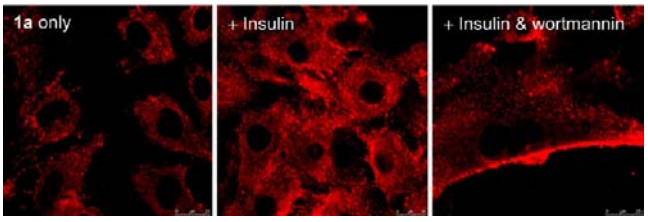

Figure 7. Laser-scanning confocal images of 3T3-L1 adipocytes upon incubation with complex **1a** (50 μM) at 37 °C for 5 min without pretreatment (left) and pretreated with insulin (100 nM, 15 min) (middle), and wortmannin (1 μM, 1 h) followed by insulin (100 nM, 15 min) (right) in a glucose-free medium, respectively.

internalized into the differentiated mouse embryonic adipocytes (3T3-L1). Interestingly, similar to the case of HeLa cells, the complex showed an elevated uptake rate toward insulin-stimulated cells, and the effect was suppressed for the cells that were pretreated with wortmannin. However, we did not observe any translocation of the complex from the tubulovesicle membranes in the cytoplasm to cell surface upon the insulin treatment.

Effects of 17β-Estradiol. The sex hormone 17β-estradiol (E2) plays an important role in the growth and progression of estrogen receptors (ER)-positive breast cancer cells.[40] Binding of E2 to ER in responsive cells such as MCF-7 cells is known to lead to growth stimulation, which requires a large amount of energy to be generated from upregulated glucose metabolism via glycolysis and the citric acid cycle.[41] We have studied the possible use of the glucose complexes to probe the metabolic changes of MCF-7 cells pretreated with E2 (30 nM) and/or its antiestrogenic agent, tamoxifen (Tam) (3 μM), for 72 h. We found that the amount of the glucose complex **1a** taken up by MCF-7 cells upon pretreatment with E2 was almost doubly increased while the galactose and sugar-free complexes **1b** and **1c**, respectively, did not show any significant differences in their uptake efficiency (Figure 8). This stimulated metabolic rate and

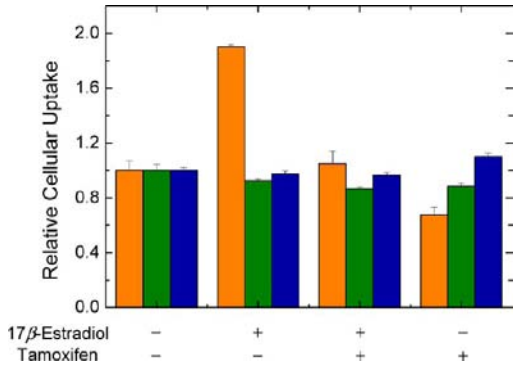

Figure 8. Relative cellular uptake of iridium associated with an average MCF-7 cell upon incubation with complexes **1a** (orange), **1b** (green), and **1c** (blue) (50 μM) at 37 °C for 5 min with or without preincubation with 17β-estradiol (30 nM) and tamoxifen (3 μM) for 72 h. The uptake of complexes **1a**−**1c** in the absence of 17β-estradiol and tamoxifen was set as respective reference points.

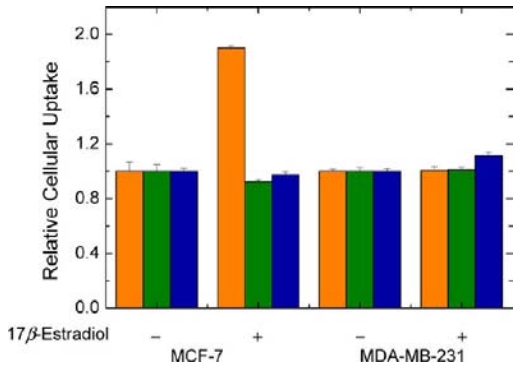

Figure 9. Relative cellular uptake of iridium associated with average MCF-7 and MDA-MB-231 cells upon incubation with complexes **1a** (orange), **1b** (green), and **1c** (blue) (50 μM) at 37 °C for 5 min with preincubation with 17β-estradiol (30 nM) for 72 h. The uptake of complexes **1a**−**1c** by the two cell lines in the absence of 17β-estradiol was set as respective reference points.

the subsequent uptake efficiency enhancement of complex **1a** was neutralized when the cells were preincubated with E2 and Tam simultaneously. In the presence of Tam alone, its antagonistic effect toward MCF-7 cells reduced the uptake of complex **1a** to *ca.* 70% (Figure 8). Again, the same treatment did not induce substantial changes to the uptake of the

dx.doi.org/10.1021/ic401714p | *Inorg. Chem.* 2013, 52, 13029−13041

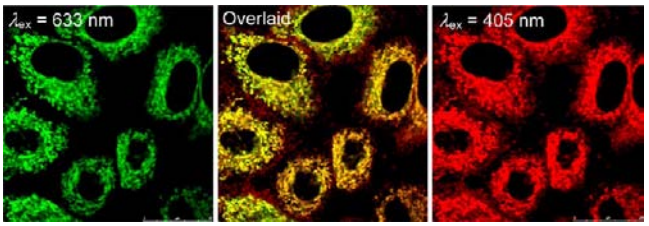

Figure 10. Laser-scanning confocal microscopy images of HeLa cells upon incubation successively with MitoTracker Deep Red FM (100 nM, 20 min, λ_{ex} = 633 nm) and complex **1a** (50 μM, 5 min, λ_{ex} = 405 nm) (Pearson's coefficient: 86%) in a glucose-free medium at 37 °C.

galactose and sugar-free complexes **1b** and **1c**, respectively. To ensure that the E2-induced enhanced uptake of the glucose complex **1a** in MCF-7 cells is due to the indirect changes of cellular glycolysis rather than an intrinsic character of the cancer cells, we have performed similar experiments using the ER-negative MDA-MB-231 breast cancer cells.[42] We found that incubation of the cells with E2 (30 nM, 72 h) prior to the treatment with complex **1a** (50 μM, 5 min) did not result in significantly increased intracellular amounts of iridium (Figure 9). Similarly, the presence of E2 did not lead to any prominent changes in the uptake of the galactose and sugar-free complexes **1b** and **1c**, respectively. Thus, the glucose complex **1a** is responsive to cellular metabolic changes, which can be exploited in the development of screening methods to study cell metabolism.

Colocalization Studies. The intracellular distribution of complex **1a** has been investigated by laser-scanning confocal microscopy. Incubation of HeLa cells with the complex resulted in effective staining of the cells. The complex was diffusely distributed in the cytoplasm with punctuate staining (Figure 4, left). The nucleus gave no emission, indicative of negligible nuclear uptake. Note that the complex was concentrated in compartments which appeared to be mitochondria. To examine the organelle-targeting properties of complex **1a**, we pretreated HeLa cells with MitoTracker Deep Red FM (100 nM, 20 min, λ_{ex} = 633 nm) before incubation with the complex (50 μM, 5 min, λ_{ex} = 405 nm). The microscopy images showed that the mitochondria were substantially costained by the fluorescent dye and the complex, with a Pearson's colocalization coefficient of 86% (Figure 10). Phosphorescent cationic and lipophilic transition metal complexes are commonly observed to stain mitochondria.[10f,26] On the basis of our recent proteomic studies of the iridium(III) isothiocyanate complex $[Ir(pq)_2(phen\text{-}NCS)]^+$,[10f] it is likely that the cytotoxicity of the complexes in this work originates from their possible interactions with proteins located at this organelle.

Photostability. Due to the high photobleaching rate of common organic dyes, their use in time-lapse imaging experiments or studies requiring prolonged irradiation is limited.[43] One of the advantages of phosphorescent transition metal complexes as biological probes is their low photobleaching rates. We have compared the photostability of the glucose complex **1a** with the commercially available fluorescent glucose-uptake indicator 2-(*N*-(7-nitrobenz-2-oxa-1,3-diazol-4-yl)-amino)-2-deoxy-D-glucose (2-NBDG).[6b] Upon laser irradiation at 488 nm (15 mW), the emission intensity of HeLa cells treated with 2-NBDG (100 μM, 5 min) was reduced much more

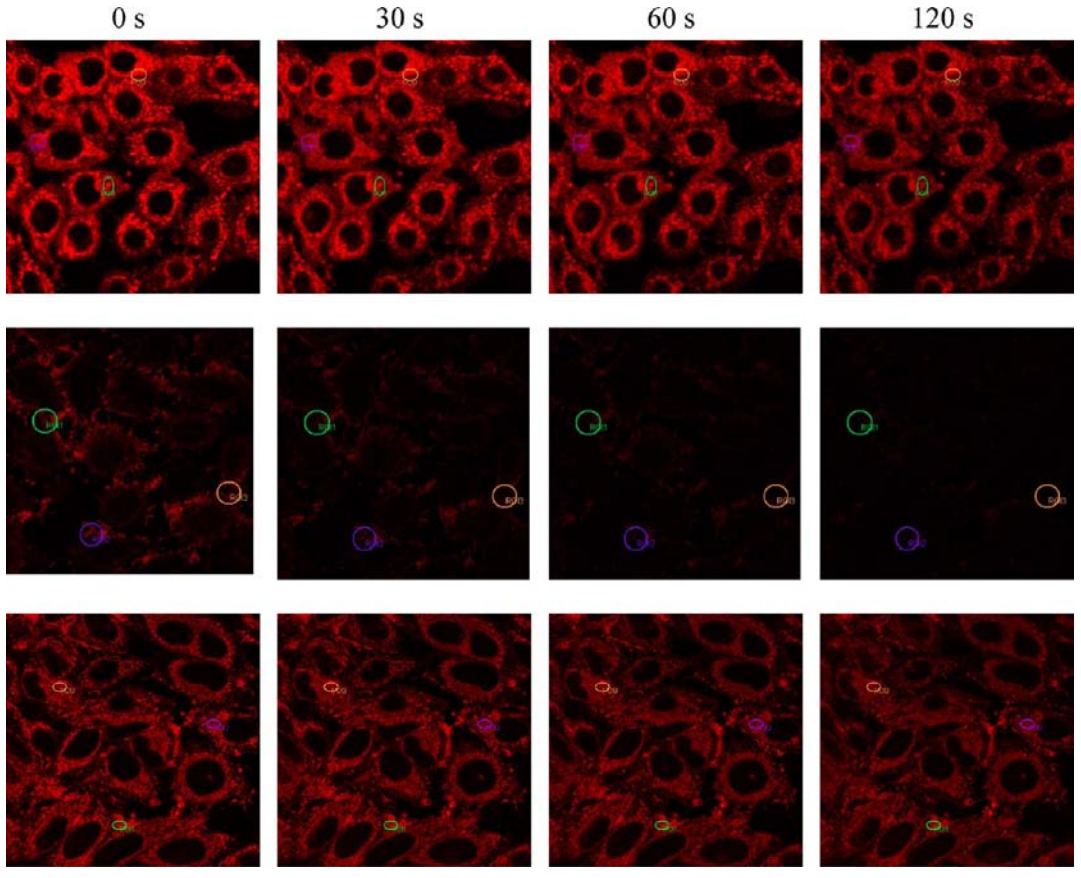

Figure 11. Laser-scanning confocal microscopy images of HeLa cells upon incubation with complex **1a** (50 μM, 5 min) (top row) and 2-NBDG (100 μM, 5 min) (middle row), and HepG2 cells upon incubation with complex **1a** (50 μM, 5 min) (bottom row), respectively, in a glucose-free medium at 37 °C under continuous exposure to laser excitation (λ_{ex} = 488 nm, power = 15 mW).

dx.doi.org/10.1021/ic401714p | *Inorg. Chem.* 2013, 52, 13029−13041

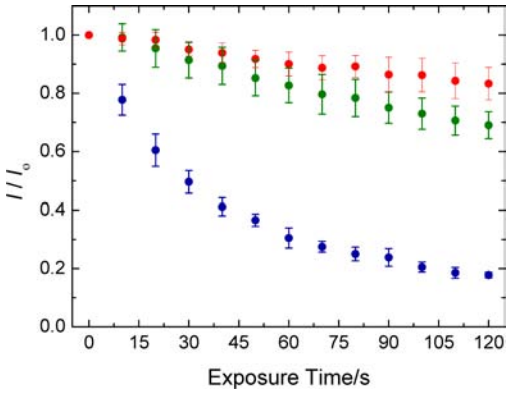

Figure 12. Changes of emission intensity of HeLa cells treated with complex **1a** (green) and 2-NBDG (blue) and HepG2 cells treated with complex **1a** (red) under continuous exposure to 488 nm (15 mW) laser excitation. The emission intensity was collected from the regions of interest shown in Figure 11, subtracted from the background fluorescence and expressed as a ratio to the initial emission intensity.

substantially compared to complex **1a** (50 μM, 5 min) (Figure 11). The emission intensity of 2-NBDG decreased to *ca.* 20% of its initial value upon continuous irradiation for 120 s. However, the emission intensity of complex **1a** was only reduced to *ca.* 70% of its initial value under the same conditions (Figure 12). A similar experiment was performed on the human hepatocellular carcinoma (HepG2). Again, prolonged irradiation only induced a *ca.* 20% drop of the emission intensity of complex **1a** (Figures 11 and 12). Thus, the high photostability indicates that the iridium(III) glucose complexes are excellent candidates for time-lapse cellular imaging applications.

CONCLUSIONS

In this work, a series of phosphorescent cyclometalated iridium(III) bipyridine glucose and galactose complexes has been synthesized, and their photophysical characteristics, lipophilicity, and cellular uptake properties have been investigated. A range of cellular experiments indicated that the uptake of the bt–glucose complex **1a** is mediated by GLUTs. The most important observation is the inhibition of uptake by D-glucose and 2-deoxy-D-glucose but not by L-glucose. Cell line dependence as well as cellular stimulation and inhibition experiments involving insulin and E2 indicated that complex **1a** potentially functions as a phosphorescent glucose uptake indicator that is also responsive toward hormonal and metabolic stimulation and inhibition to the cells. Although hexokinase assays did not reveal any phosphorylation of complex **1a**, confocal microscopy indicated that the complex is localized in the mitochondria, which is a result of its cationic and lipophilic nature. Additionally, prolonged irradiation of the complex showed that its photostability is much higher than that of the fluorescent organic compound 2-NBDG. It is conceivable that this class of iridium(III) bipyridine glucose complexes will offer new insight in the development of phosphorescent glucose uptake indicators and screening methods to study cell metabolism. Related studies on phosphorescent inorganic and organometallic transition metal sugar conjugates are underway.

ASSOCIATED CONTENT

Supporting Information

ESI-MS and ^{1}H NMR spectra of the iridium(III) complexes, and confocal microscopy images of complex **1b**. This material is available free of charge via the Internet at http://pubs.acs.org.

AUTHOR INFORMATION

Corresponding Author

*E-mail: bhkenlo@cityu.edu.hk. Phone: (852) 3442 7231. Fax: (852) 3442 0522.

Notes

The authors declare no competing financial interest.

ACKNOWLEDGMENTS

We thank the Hong Kong University Grants Committee Areas of Excellence Scheme (AoE/P-03/08) and Hong Kong Research Grants Council (Projects CityU 102212 and CityU 102311) for financial support. W.H.-T.L. acknowledges the receipt of a Postgraduate Studentship, a Research Tuition Scholarship, and an Outstanding Academic Performance Award administrated by City University of Hong Kong. We thank Dr. Hiu-Yee Kwan of the Hong Kong Baptist University for her generous gift of 3T3-L1 cells and Mr. Kenneth King-Kwan Lau, Mr. Michael Wai-Lun Chiang, and Mr. Ho-Hang Chan for their assistance on the cellular experiments.

REFERENCES

(1) (a) Clark, D. D.; Sokloff, L. *Basic Neurochemistry: Molecular, Cellular and Medical Aspects*; Lippincott: Philadelphia, 1999. (b) Garrett, R. H.; Grisham, C. M. *Biochemistry*; Saunders College Publishing, Orlando, FL, 1999. (c) Medina, R. A.; Owen, G. I. *Biol. Res.* **2002**, *35*, 9–26. (d) Zhao, F.-Q.; Keating, A. F. *Curr. Genomics* **2007**, *8*, 113–128. (e) Nualart, F.; Los Angeles García, M.; Medina, R. A.; Owen, G. I. *Curr. Vasc. Pharmacol.* **2009**, *7*, 534–548.

(2) (a) McAllister, M. S.; Krizance-Bengez, L.; Macchia, F.; Naftalin, R. J.; Pedley, K. C.; Mayberg, M. R.; Marroni, M.; Leaman, S.; Stanness, K. A.; Janigro, D. *Brain Res.* **2001**, *904*, 20–30. (b) Wood, I. S.; Trayhurn, P. *Br. J. Nutr.* **2003**, *89*, 3–9. (c) Brown, M. L.; Orvig, C. *Chem. Commun.* **2008**, 5077–5091.

(3) (a) Warburg, O. *Science* **1956**, *123*, 309–314. (b) Aloj, L.; Caracó, C.; Jagoda, E.; Eckelman, W. C.; Neumann, R. D. *Cancer Res.* **1999**, *59*, 4709–4714. (c) Nakashima, R. A.; Paggi, M. G.; Pedersen, P. L. *Cancer Res.* **1984**, *44*, 5702–5706. (d) Rudlowski, C.; Moser, M.; Becker, A. J.; Rath, W.; Buttner, R.; Schroder, W.; Schurmann, A. *Oncology* **2004**, *66*, 404–410. (e) Macheda, M. L.; Rogers, S.; Best, J. D. *J. Cell. Physiol.* **2005**, *202*, 654–662.

(4) (a) Son, P.; Atkins, H. L.; Bandoypadhyay, D.; Fowler, J. S.; MacGregor, R. R.; Matsui, K.; Oster, Z. H.; Sacker, D. F.; Shiue, C. Y.; Turner, H.; Wan, C. N.; Wolf, A. P.; Zabinski, S. V. *J. Nucl. Med.* **1980**, *21*, 670–675. (b) Conti, P. S.; Liken, D. L.; Hawley, K.; Keppler, J.; Grafton, S. T.; Buding, J. R. *Nucl. Med. Biol.* **1996**, *23*, 717–735. (c) Beuthien-Baumann, B.; Hamacher, K.; Oberdorfer, F.; Steinbach, J. *Carbohydr. Res.* **2000**, *327*, 107–118. (d) Krohn, K. A.; Mankoff, D. A.; Muzi, M.; Link, J. M.; Spence, A. M. *Nucl. Med. Biol.* **2005**, *32*, 663–671.

(5) Kee, W. H.; Lee, J.; Jung, D.-W.; Williams, D. R. *Sensors* **2012**, *12*, 5005–5027.

(6) (a) Lartey, P. A.; Derechin, M. *Prep. Biochem.* **1979**, *9*, 85–95. (b) Yoshioka, K.; Takahashi, H.; Homma, T.; Saito, M.; Oh, K.-B.; Nemoto, Y.; Matsuoka, H. *Biochem. Biophys. Acta* **1996**, *1289*, 5–9. (c) Yoshioka, K.; Saito, M.; Oh, K.-B.; Nemoto, Y.; Matsuoka, H.; Natsume, M.; Abe, H. *Biosci., Biotechnol., Biochem.* **1996**, *60*, 1899–1901. (d) Park, J.; Lee, H. Y.; Cho, M.-H.; Park, S. B. *Angew. Chem., Int. Ed.* **2007**, *46*, 2018–2022. (e) Lee, H.; Lee, J. J.; Park, J.; Park, S. B. *Chem.—Eur. J.* **2011**, *17*, 143–150.

(7) (a) Cheng, Z.; Ievi, J.; Xiong, Z.; Gheysens, O.; Keren, S.; Chen, X.; Gambhir, S. S. *Bioconjugate Chem.* **2006**, *17*, 662–669. (b) Kovar, J.; Volcheck, W.; Sevick-Muraca, E.; Simpson, M. A.; Olive, D. M. *Anal. Biochem.* **2009**, *384*, 254–262. (c) Vendrell, M.; Samanta, A.; Yun, S.-W.; Chang, Y.-T. *Org. Biomol. Chem.* **2011**, *9*, 4760–4762. (d) Zhang, M.; Zhang, Z.; Blessington, D.; Li, H.; Busch, T. M.; Madrak, V.; Miles, J.; Chance, B.; Glichson, J. D.; Zheng, G.

Bioconjugate Chem. **2003**, *14*, 709−714. (e) Tian, Y. S.; Lee, H. Y.; Lim, C. S.; Park, J.; Kim, H. M.; Shin, Y. N.; Kim, E. S.; Jeon, H. J.; Park, S. B.; Cho, B. R. *Angew. Chem., Int. Ed.* **2009**, *48*, 8027−8031.
(8) See, for example: (a) Petrig, J.; Schibli, R.; Dumas, C.; Alberto, R.; Schubiger, P. A. *Chem.—Eur. J.* **2001**, *7*, 1868−1873. (b) Storr, T.; Obata, M.; Fisher, C. L.; Bayly, S. R.; Green, D. E.; Brudziñska, I.; Mikata, Y.; Patrick, B. O.; Adam, M. J.; Yano, S.; Orvig, C. *Chem.—Eur. J.* **2005**, *11*, 195−203. (c) Storr, T.; Sugai, Y.; Barta, C. A.; Mikata, Y.; Adam, M. J.; Yano, S.; Orvig, C. *Inorg. Chem.* **2005**, *44*, 2698−2705. (d) Ferreira, C. L.; Ewart, C. B.; Bayly, S. R.; Patrick, B. O.; Steele, J.; Adam, M. J.; Orvig, C. *Inorg. Chem.* **2006**, *45*, 6979−6987. (e) Schibli, R.; Dumas, C.; Petrig, J.; Spadola, L.; Scapozza, L.; Garcia-Garayoa, E.; Schubiger, P. A. *Bioconjugate Chem.* **2005**, *16*, 105−112. (f) Bowen, M. L.; Lim, N. C.; Ewart, C. B.; Misri, R.; Ferreira, C. L.; Häfeli, U.; Adam, M. J.; Orvig, C. *Dalton Trans.* **2009**, 9216−9227. (g) Ferreira, C. L.; Marques, F. L. N.; Okamoto, M. R. Y.; Otake, A. H.; Sugai, Y.; Mikata, Y.; Storr, T.; Bowen, M.; Yano, S.; Adam, M. J.; Chammas, R.; Orvig, C. *Appl. Radiat. Isot.* **2010**, *68*, 1087−1093. (h) Iqbal, M. S.; Khurshid, S. J.; Muhammad, B. *Med. Chem. Res.* **2013**, *22*, 861−868.
(9) See, for example: (a) Hasegawa, T.; Yonemura, T.; Matsuura, K.; Kobayashi, K. *Bioconjugate Chem.* **2003**, *14*, 728−737. (b) Banerjee, S. R.; Babich, J. W.; Zubieta, J. *Inorg. Chim. Acta* **2006**, *359*, 1603−1612. (c) Gottschaldt, M.; Schubert, U. S.; Rau, S.; Yano, S.; Vos, J. G.; Kroll, T.; Clement, J.; Hilger, I. *ChemBioChem* **2010**, *11*, 649−652. (d) Li, M.-J.; Jiao, P.; He, W.; Yi, C.; Li, C.-W.; Chen, X.; Chen, G.-N.; Yang, M. *Eur. J. Inorg. Chem.* **2011**, 197−200. (e) Louie, M.-W.; Liu, H.-W.; Lam, M. H.-C.; Lo, K. K.-W. *Chem.—Eur. J.* **2011**, *17*, 8304−8308. (f) Lo, K. K.-W.; Law, W. H.-T.; Chan, J. C.-Y.; Liu, H.-W.; Zhang, K. Y. *Metallomics* **2013**, *5*, 808−812. (g) Zhang, K. Y.; Tso, K. K.-S.; Louie, M.-W.; Liu, H.-W.; Lo, K. K.-W. *Organometallics* **2013**, *32*, 5098−5102.
(10) (a) Zhang, K. Y.; Li, S. P.-Y.; Zhu, N.; Or, I. W.-S.; Cheung, M. S.-H.; Lam, Y.-W.; Lo, K. K.-W. *Inorg. Chem.* **2010**, *49*, 2530−2540. (b) Li, S. P.-Y.; Liu, H.-W.; Zhang, K. Y.; Lo, K. K.-W. *Chem.—Eur. J.* **2010**, *16*, 8329−8339. (c) Liu, H.-W.; Zhang, K. Y.; Law, W. H.-T.; Lo, K. K.-W. *Organometallics* **2010**, *29*, 3474−3476. (d) Lee, P.-K.; Law, W. H.-T.; Liu, H.-W.; Lo, K. K.-W. *Inorg. Chem.* **2011**, *50*, 8570−8579. (e) Li, S. P.-Y.; Tang, T. S.-M.; Yiu, K. S.-M.; Lo, K. K.-W. *Chem.—Eur. J.* **2012**, *18*, 13342−13354. (f) Wang, B.; Liang, Y.; Dong, H.; Tan, T.; Zhan, B.; Cheng, J.; Lo, K. K.-W.; Lam, Y.-W.; Cheng, S.-H. *ChemBioChem* **2012**, *13*, 2729−2737. (g) Lo, K. K.-W.; Chan, B. T.-K.; Liu, H.-W.; Zhang, K. Y.; Li, S. P.-Y.; Tang, T. S.-M. *Chem. Commun.* **2013**, *49*, 4271−4273. (h) Li, S. P.-Y.; Lau, C. T.-S.; Louie, M.-W.; Lam, Y.-W.; Cheng, S.-H.; Lo, K. K.-W. *Biomaterials* **2013**, *34*, 7519−7532.
(11) Perrin, D. D.; Armarego, W. L. F. *Purification of Laboratory Chemicals*; Elsevier: Oxford, U.K., 2009.
(12) Sprous, S.; King, K. A.; Spellane, P. J.; Watts, R. J. *J. Am. Chem. Soc.* **1984**, *106*, 6647−6653.
(13) Zhang, K. Y.; Lo, K. K.-W. *Inorg. Chem.* **2009**, *48*, 6011−6025.
(14) Demas, J. N.; Crosby, G. A. *J. Phys. Chem.* **1971**, *75*, 991−1024.
(15) Nakamura, K. *Bull. Chem. Soc. Jpn.* **1982**, *55*, 2697−2705.
(16) Minick, D. J.; Frenz, J. H.; Patrick, M. A.; Brent, D. A. *J. Med. Chem.* **1988**, *31*, 1923−1933.
(17) (a) Lo, K. K.-W.; Chung, C.-K.; Lee, T. K.-M.; Lui, L.-H.; Tsang, K. H.-K.; Zhu, N. *Inorg. Chem.* **2003**, *42*, 6886−6897. (b) Lo, K. K.-W.; Chan, J. S.-W.; Lui, L.-H.; Chung, C.-K. *Organometallics* **2004**, *23*, 3108−3116. (c) Lo, K. K.-W.; Zhang, K. Y.; Chung, C.-K.; Kwok, K. Y. *Chem.—Eur. J.* **2007**, *13*, 7110−7120. (d) Lau, J. S.-Y.; Lee, P.-K.; Tsang, K. H.-K.; Ng, C. H.-C.; Lam, Y.-W.; Cheng, S.-H.; Lo, K. K.-W. *Inorg. Chem.* **2009**, *48*, 708−718.
(18) Lo, K. K.-W.; Li, C.-K.; Lau, J. S.-Y. *Organometallics* **2005**, *24*, 4594−4601.
(19) Oldfield, S. P.; Hall, M. D.; Platts, J. A. *J. Med. Chem.* **2007**, *50*, 5227−5237.
(20) (a) Lo, K. K.-W.; Lee, P.-K.; Lau, J. S.-Y. *Organometallics* **2008**, *27*, 2998−3006. (b) Zhang, K. Y.; Liu, H.-W.; Fong, T. T.-H.; Chen, X.-G.; Lo, K. K.-W. *Inorg. Chem.* **2010**, *49*, 5432−5443.
(21) VanBrocklin, H. F.; Liu, A.; Welch, M. J.; O'Neil, J. P.; Katzenellenbogen, J. A. *Steroids* **1994**, *59*, 34−45.
(22) (a) Wright, E. M. *Annu. Rev. Physiol.* **1993**, *55*, 575−589. (b) Cohen, N. R.; Knecht, D. A.; Lodish, H. F. *Biochem. J.* **1996**, *315*, 971−975. (c) Manolescu, A. R.; Witkowska, K.; Kinnaird, A.; Cessford, T.; Cheeseman, C. *Physiology* **2007**, *22*, 234−240. (d) Carruthers, A.; DeZutter, J.; Ganguly, A.; Devaskar, S. U. *Am. J. Physiol.: Endocrinol. Metab.* **2009**, *297*, E836−E848.
(23) Ismail-Beigi, F. *J. Membr. Biol.* **1993**, *135*, 1−10.
(24) Mosmann, T. J. *Immunol. Methods* **1983**, *65*, 55−63.
(25) Leung, S.-K.; Liu, H.-W.; Lo, K. K.-W. *Chem. Commun.* **2011**, *47*, 10548−10550.
(26) Pisani, M. J.; Weber, D. K.; Heimann, K.; Collins, J. G.; Keene, F. R. *Metallomics* **2010**, *2*, 393−396.
(27) (a) Dautry-Varsat, A.; Ciechanover, A.; Lodish, H. F. *Proc. Natl. Acad. Sci. U.S.A.* **1983**, *80*, 2258−2262. (b) Reaven, E.; Tsai, L.; Azhar, S. *J. Biol. Chem.* **1996**, *271*, 16208−16217. (c) Weaver, D. J., Jr.; Voss, E. W., Jr. *Biol. Cell.* **1998**, *90*, 169−181.
(28) (a) Shetty, M.; Loeb, J. N.; Vikstrom, K.; Ismail-Beigi, F. *J. Biol. Chem.* **1993**, *268*, 17225−17232. (b) Behrooz, A.; Ismail-Beigi, F. *J. Biol. Chem.* **1997**, *272*, 5555−5562.
(29) Wang, G. L.; Semenza, G. L. *Proc. Natl. Acad. U.S.A.* **1993**, *90*, 4304−4308.
(30) (a) Rabuazzo, A. M.; Buscema, M.; Vinci, C.; Caltabiano, V.; Anello, M.; Vigneri, R.; Purrello, F. *Diabetologia* **1993**, *36*, 1204−1207. (b) Ojeda, P.; Pérez, A.; Ojeda, L.; Vargas-Uribe, M.; Rivas, C. I.; Salas, M.; Vera, J. C.; Reyes, A. M. *Am. J. Physiol.* **2012**, *303*, C530−C539.
(31) Wood, T. E.; Dalili, S.; Simpson, C. D.; Hurren, R.; Mao, X.; Saiz, F. S.; Gronda, M.; Eberhard, Y.; Minden, M. D.; Bilan, P. J.; Klip, A.; Batey, R. A.; Schimmer, A. *Mol. Cancer Ther.* **2008**, *7*, 3546−3555.
(32) Speizer, L.; Haugland, R.; Kutchai, H. *Biochim. Biophys. Acta, Biomembr.* **1985**, *815*, 75−84.
(33) (a) Rempel, A.; Mathupala, S. P.; Pedersen, P. L. *FEBS Lett.* **1996**, *385*, 233−237. (b) Younes, M.; Lechago, L. V.; Somoano, J. R.; Mosharaf, M.; Lechago, J. *Cancer Res.* **1996**, *56*, 1164−1167. (c) Chung, J.-K.; Lee, Y. J.; Kim, C.; Choi, S. R.; Kim, M.; Lee, K.; Jeong, J. M.; Lee, D. S.; Jang, J.-J.; Lee, M. C. *J. Nucl. Med.* **1999**, *40*, 339−346. (d) Aft, R. L.; Zhang, F. W.; Gius, D. *Br. J. Cancer* **2002**, *87*, 805−812. (e) Gatenby, R. A.; Gillies, R. J. *Nat. Rev. Cancer* **2004**, *4*, 891−899. (f) Jin, Q.; Agrawal, L.; VanHorn-Ali, Z.; Alkhatib, G. *Virology* **2006**, *349*, 184−196. (g) Gillies, R. J.; Robey, I.; Gatenby, R. A. *J. Nucl. Med.* **2008**, *49*, 24S−42S. (h) Rodríguez-Enríquez, S.; Marín-Hernández, A.; Gallardo-Pérez, J. C.; Carreño-Fuentes, L.; Moreno-Sánchez, R. *Mol. Nutr. Food Res.* **2009**, *53*, 29−48.
(34) (a) Yushok, W. D. *Cancer Res.* **1964**, *24*, 187−192. (b) Panneman, H.; Ruijter, G. J. G.; van den Broeck, H. C.; Visser, J. *Eur. J. Biochem.* **1998**, *258*, 223−232.
(35) Bessell, E. M.; Foster, A. B.; Westwood, J. H. *Biochem. J.* **1972**, *128*, 199−204.
(36) (a) Ferrannini, E.; Santoro, D.; Bonadonna, R.; Natali, A.; Parodi, O.; Camici, P. G. *Am. J. Physiol.: Endocrinol. Metab.* **1993**, *264*, E308−E315. (b) Krusznska, Y. T.; Ciaraldi, T. P.; Henry, R. R. *Compr. Physiol.* **2011**, 579−607. (c) Bergandi, L.; Silvagno, F.; Russo, I.; Riganti, C.; Anfossi, G.; Aldieri, E.; Ghigo, D.; Trovati, M.; Bosia, A. *Arterioscler., Thromb., Vasc. Biol.* **2003**, *23*, 2215−2221. (d) Calvo, M. B.; Figueroa, A.; Pulido, E. G.; Campelo, R. G.; Aparicio, L. A. *Int. J. Endocrinol.* **2010**, 1−14.
(37) (a) Stephen, N. S.; Harold, A. *Biochem. Biophys. Res. Commun.* **1973**, *53*, 357−365. (b) Ding, X.-Z.; Fehsenfeld, D. M.; Murphy, L. O.; Permert, J.; Adrain, T. E. *Pancreas* **2000**, *21*, 310−320. (c) Singh, A.; Purohit, A.; Hejaz, H. A. M.; Potter, B. V. L; Reed, M. J. *J. Mol. Cell. Endocrinol.* **2000**, *160*, 61−66.
(38) Note that insulin-sensitive uptake of galactose has been documented. See, for example: (a) Nakada, H. I.; Wick, A. N. *Am. J. Physiol.* **1956**, *185*, 23−26. (b) Levari, R.; Kornblueth, W.; Wertheimer, E. *J. Endocrinol.* **1961**, *22*, 361−369. (c) Lotspeich, W. D.; Wheeler, A. H. *Am. J. Physiol.* **1962**, *202*, 1065−1069. (d) Vega, F. V.; Kono, T. *Biochim. Biophys. Acta, Biomembr.* **1978**, *512*, 221−222.
(39) (a) Clarke, J. F.; Young, P. W.; Yonezawa, K.; Kasuga, M.; Holman, G. D. *Biochem. J.* **1994**, *300*, 631−635. (b) Egert, S.; Nguyen, N.; Brosius, F. C., III; Schwaiger, M. *Cardiovasc. Res.* **1997**, *35*, 283−293. (c) Nedachi,

T.; Kanzaki, M. *Am. J. Physiol.: Endocrinol. Metab.* **2006**, *291*, E817−E828.
(40) (a) Arfah, B. M.; Griffin, P.; Gordon, N. H.; Pearson, O. H. *Cancer Res.* **1986**, *46*, 3268−3272. (b) Neeman, M.; Hadassa, D. *Cancer Res.* **1989**, *49*, 589−594. (c) Yager, J. D.; Davidson, N. E. *N. Engl. J. Med.* **2006**, *354*, 270−282.
(41) (a) Nararsimhan, T. R.; Safe, S.; Williams, H. J.; Scott, A. I. *Mol. Pharmacol.* **1991**, *40*, 1029−1035. (b) Furman, E.; Rushkin, E.; Margalit, R.; Bendel, P.; Degani, H. *J. Steroid Biochem. Mol. Biol.* **1992**, *43*, 189−195. (c) Rivenzon-Segal, D.; Boldin-Adamsky, S.; Seger, D.; Seger, R.; Degani, H. *Int. J. Cancer* **2003**, *107*, 177−182.
(42) Millon, S. R.; Ostrander, J. H.; Brown, J. Q.; Raheja, A.; Seewaldt, V. L.; Ramanujam, N. *Breast Cancer Res. Treat.* **2011**, *126*, 55−62.
(43) (a) O'Neil, R. G.; Wu, L.; Mullai, N. *Mol. Imaging Biol.* **2005**, *7*, 388−392. (b) Barros, L. F.; Courjaret, R.; Jakoby, P.; Loaiza, A.; Lohr, C.; Deitmer, J. W. *Glia* **2009**, *57*, 962−970.